cell and allowed to warm to ambient temperature. Argon was admitted to the bulb via the stopcock at a rate of approximately 30 cm^3 s^{-1}, bubbled through the reaction mixture, and used to carry PNA vapor through the cell.

Vapor samples for mass spectral analysis were handled similarly, except that the argon flow was eliminated. Evolution of oxygen from decomposition of PNA in the reaction mixture was sufficient to sweep PNA vapors into the system. The mass spectrometer and inlet system have been described elsewhere.[24]

The evolution of oxygen from aqueous PNA solutions was monitored with a calibrated pressure transducer (Validyne model DP-7) connected via a three-way stopcock to a jacketed, 250-mL bulb equipped with magnetic sitrrer. To perform the experiments, we added 100.0 mL of buffer to the bulb and allowed the mixture to come to reaction temperature while O_2 was vigorously bubbled through the solution. Next, the O_2 flow was stopped, 25-100 μL of a PNA reaction mixture were added via syringe, the stopcock closed, and transducer output monitored with a strip chart recorder. For a 50-μL aliquot of preparative method 2, assuming 100% yield of PNA, the initial PNA concentration in 100 mL of buffer is calculated to be 7.5×10^{-4} M. For a 150-cm^3 gas volume, the final pressure of the system is calculated to be 9 torr, assuming complete decomposition to O_2. Consistent with these calculations, observed final pressures were typically 5-10 torr. Control experiments indicated significant oxygen evolution from excess H_2O_2 for PNA decompositions when preparative method 2 was used and pH ≤4. To circumvent this problem, we adopted preparative method 3, which does not require a large excess of H_2O_2.

Oxygen was identified as the reaction product by allowing a sample of PNA to decompose in a sealed, degassed tube and then analyzing the gas over the frozen solution by mass spectroscopy.

Nitrite evolution was followed by monitoring the absorption at 365 nm with a Perkin-Elmer model 554 spectrophotometer. The buffer solution was first equilibrated to the desired temperature and 50-100 μL of PNA solution was then injected into the buffer and mixed well. The absorbance at 365 nm was monitored until completion of the reaction.

(24) Chang, J. S.; Barker, J. R.; Davenport, J. E.; Golden, D. M. *Chem. Phys. Lett.* **1979**, *60*, 385.

Acknowledgment. We gratefully acknowledge Dr. John R. Barker (SRI International) and Professor Mario Molina (University of California, Irvine) for their helpful discussions. This work was supported in part by DOT/FAA Contract No. DOT-FA78 WA-4228.

Insertion of Carbon Monoxide into Metal-Nitrogen Bonds. Synthesis, Chemistry, Structures, and Structural Dynamics of Bis(pentamethylcyclopentadienyl) Organoactinide Dialkylamides and η^2-Carbamoyls

Paul J. Fagan,[1a] Juan M. Manriquez,[1a] Sarah H. Vollmer,[1b] Cynthia Secaur Day,[1c] Victor W. Day,*[1b,d] and Tobin J. Marks*[1a,d]

Contribution from the Departments of Chemistry, Northwestern University, Evanston, Illinois 60201, and University of Nebraska, Lincoln, Nebraska 68588, and Crystalytics Company, Lincoln, Nebraska 68501. *Received August 27, 1979*

Abstract: This paper reports the synthesis and characterization of chlorobis(pentamethylcyclopentadienyl)thorium and -uranium dialkylamides, $M[\eta\text{-}(CH_3)_5C_5]_2(NR_2)Cl$ (M = Th, U; R = CH_3, C_2H_5), and bis(dialkylamides), $M[\eta\text{-}(CH_3)_5C_5]_2(NR_2)_2$ (M = Th, U, R = CH_3; M = U, R = C_2H_5). NMR studies indicate restricted rotation about the M-NR_2 bonds. The amide compounds undergo facile migratory insertion of carbon monoxide to produce the corresponding η^2-carbamoyl complexes $M[\eta\text{-}(CH_3)_5C_5]_2[\eta^2\text{-}CONR_2]Cl$, $M[\eta\text{-}(CH_3)_5C_5]_2[\eta^2\text{-}CONR_2]NR_2$, and $M[\eta\text{-}(CH_3)_5C_5]_2[\eta^2\text{-}CONR_2]_2$ which were characterized by a variety of chemical and physicochemical methods. The infrared spectra of these compounds exhibit unusually low C-O stretching frequencies (1490-1560 cm^{-1}) for carbamoyl complexes, indicative of strong metal-oxygen bonding. The molecular structures of $Th[\eta\text{-}(CH_3)_5C_5]_2[\eta^2\text{-}CON(C_2H_5)_2]Cl$ and $U[\eta\text{-}(CH_3)_5C_5]_2[\eta^2\text{-}CON(CH_3)_2]_2$ have been determined by single-crystal X-ray diffraction techniques. The former complex crystallizes in the monoclinic space group $P2_1/n$ (an alternate setting of $P2_1/c$—C_{2h}^5) with four molecules in a cell of dimensions: a = 9.097 (2) Å, b = 21.291 (4) Å, c = 14.031 (2) Å, and β = 95.78 (2)°; the latter complex crystallizes in the monoclinic space group $P2_1/c$—C_{2h}^5 with four molecules in a unit cell of dimensions: a = 9.277 (4) Å, b = 16.143 (5) Å, c = 18.977 (6) Å, and β = 130.55 (3)°. For the chloro complex, least-squares refinement led to a value for the conventional R index (on F) of 0.080 for 3156 independent reflections having $2\theta_{MoK\bar{\alpha}} < 55°$ and $I > 3\sigma(I)$, while for the bis(carbamoyl), least-squares refinement led to a conventional R (on F) of 0.036 for 3689 independent reflections having $2\theta_{MoK\bar{\alpha}} < 55°$ and $I > 3\sigma(I)$. The $M[(CH_3)_5C_5]_2$ fragments of both molecules are of the "bent sandwich" $M(C_5H_5)_2X_2$ configuration, with the carbamoyl ligands bound in a η^2 fashion. The chloro complex is disordered, with two isomers (one with the C-O vector pointing toward the Cl atom, one with it pointing away) having cocrystallized in nearly equal proportions. The Th-O distances are 2.383 (31) and 2.460 (16) Å; the average Th-C distance is 2.418 (20) Å; the Th-C-O angles accompanying the above distances are 70.1 (15) and 74.5 (1)°, respectively. In solution, the two isomers of the analogous uranium complex are in equilibrium (ΔH = 1.2 ± 0.1 kcal/mol; ΔS = 8 ± 1 eu) with interconversion rapid on the ^1H NMR time scale at room temperature (at -80 °C, $\Delta G^{\ddagger}$ = 8.9 ± 0.5 kcal/mol). In the bis(carbamoyl), the U-O distances are 2.370 (5) and 2.342 (7) Å, the corresponding U-C distances 2.405 (8) and 2.402 (9) Å, and the corresponding U-C-O angles 73.0 (4) and 71.8 (5)°. The structural and spectral data evidence dative nitrogen lone-pair donation to the "carbenoid" carbamoyl carbon atom. The complex $Th[\eta\text{-}(CH_3)_5C_5]_2[N(CH_3)_2]CH_3$ was also prepared; carbonylation occurs preferentially at the metal-carbon bond to yield $Th[\eta\text{-}(CH_3)_5C_5]_2[N(CH_3)_2](\eta^2\text{-}COCH_3)$.

The classic migratory insertion reaction of carbon monoxide into a two-center, two-electron metal-carbon bond (eq 1, X = a hydrocarbyl functionality) is an extremely important transformation in stoichiometric and catalytic organometallic chemistry.[2]

0002-7863/81/1503-2206$01.25/0

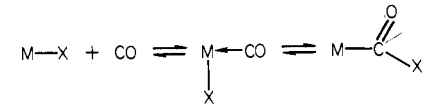

(1)

Although a great many aspects of this CO activation process are now well understood, it is not at present clear that a picture evolved solely from results on "soft" mononuclear transition-metal complexes is entirely accurate or complete in describing the rather drastic processes by which hydrogenation, deoxygenation, and/or homologation of the CO molecule are occurring[3] (especially under heterogeneous Fischer–Tropsch, methanation, and alcohol synthesis conditions). This question has led to the search for new modes of CO reactivity, and significant attention has recently focused on organometallic complexes of early transition metals[4,5] and actinides.[6,7] The latter offered us the possibility of exploring CO activation patterns at unusual molecular sites which might have characteristics similar to heterogeneous CO reduction environments: high coordinative unsaturation and high oxygen affinity.[3,8]

We recently reported that actinide hydrocarbyl CO activation involves the formation of highly reactive η^2-acyls (eq 2, X = a

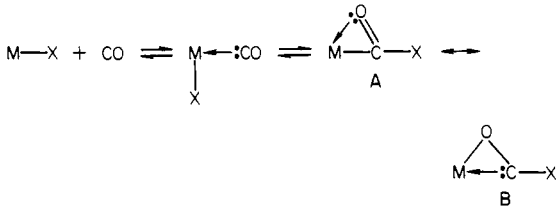

A

B

(2)

hydrocarbyl functionality), and that in these species there is considerable perturbation of the insertion product ligation toward an oxycarbenoid structure (B) in which strong metal–oxygen bonding takes place.[6,7] For Th[η-$(CH_3)_5C_5$]$_2$[η^2-$COCH_2C(CH_3)_3$]Cl (C) the Th–O bond distance is only slightly longer than

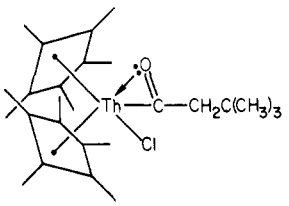

C

a Th–O single bond distance (2.37 (2)[7a] vs. 2.154 (8) Å[7b]) and ν_{CO} falls to 1469 cm^{-1}.[7a] Such observations have important consequences in understanding the general constraints under which CO insertion into metal–element bonds takes place. Viewed thermodynamically in terms of the strengths of the bonds being made and broken, the favorability of eq 1 should be strongly correlated with the relatively large variations expected in the M–X bond energies,[9,10] while for most X, the variations in insertion product M–C and C–X bond energies should be appreciably smaller.[9,10] As an illustration, metal–carbon σ bonds are relatively weak, and CO insertion is facile.[2] On the other hand, there is accumulating evidence that metal–hydrogen bond energies are greater[11] and that for most metals, formyl production via CO migratory insertion (eq 1, X = H) is relatively unfavorable.[12,13] A plausible way to circumvent such constraints may exist in coordination environments where ancillary intramolecular metal–oxygen bonding stabilizes the insertion product (eq 2). For example, it is likely that Th–O mean bond dissociation energies exceed Th–C mean bond dissociation energies by ca. 50 kcal/mol or more,[14] and judging from the aforementioned Th-[$(CH_3)_5C_5$]$_2$[η^2-$COCH_2C(CH_3)_3$]Cl metrical data, the metal–oxygen interaction[15] significantly stabilizes the insertion product in this complex. In fact, this interaction appears to be stronger than in the analogous $Zr(C_5H_5)_2(\eta^2\text{-COR})R$ complexes[4b,16] and may explain why the latter complexes readily undergo thermal decarbonylation while the thorium compound does not.[7a,17] In broader terms, such metal–oxygen interactions may promote and allow the study of CO activation processes which have not been previously observed in solution under normal conditions and which may be important under other (e.g., heterogeneous) conditions.

(1) (a) Northwestern University. (b) University of Nebraska. (c) Crystalytics Co. (d) Camille and Henry Dreyfus Teacher-Scholar.

(2) (a) Parshall, G. W. "Homogeneous Catalysis"; Wiley-Interscience: New York, 1980; Chapter 5. (b) Eisenberg, R.; Hendricksen, D. E. *Adv. Catal.* **1979**, *28*, 79–172. (c) Heck, R. F. "Organotransition Metal Chemistry"; Academic Press: New York, 1974; Chapter IX. (d) Wojcicki, A. *Adv. Organomet. Chem.* **1973**, *11*, 87–145.

(3) (a) Muetterties, E. L.; Stein, J. *Chem. Rev.* **1979**, *79*, 479–490. (b) Masters, C. *Adv. Organomet. Chem.* **1979**, *17*, 61–103. (c) Denny, P. J.; Whan, D. A. *Catalysis (London)* **1978**, *2*, 46–86. (d) Ponec, V. *Catal. Rev.—Sci. Eng.* **1978**, *18*, 151–171. (e) Schulz, H. J. *Erdoel Kohle, Erdgas, Petrochem.* **1977**, *30*, 123–131. (f) Henrici-Olivè, G.; Olivè, S. *Angew. Chem. Int. Ed., Engl.* **1976**, *15*, 136–141. (g) Vannice, M. A. *Catal. Rev.—Sci. Eng.* **1976**, *14*, 153–191 and references therein.

(4) (a) Wolczanski, P. T.; Bercaw, J. E. *Acc. Chem. Res.* **1980**, *13*, 121–127 and references therein. (b) Calderazzo, F. *Angew. Chem., Int. Ed. Engl.* **1977**, *16*, 299–311 and references therein. (c) Lauher, J. W.; Hoffman, R. *J. Am. Chem. Soc.* **1976**, *98*, 1729–1742.

(5) (a) Marsella, J. A.; Caulton, K. G. *J. Am. Chem. Soc.* **1980**, *102*, 1747–1748. (b) Lappert, M. F.; Juong-Thi, N. T.; Milne, C. R. C. *J. Organomet. Chem.* **1979**, *74*, C35–C37. (c) Wood, C. D.; Schrock, R. R. *J. Am. Chem. Soc.* **1979**, *101*, 5421–5422. (d) Labinger, J. A.; Wong, K. S.; Scheidt, R. *Ibid.* **1978**, *100*, 3254–3255. (e) Bercaw, J. E. *Adv. Chem. Ser.* **1978**, *No. 167*, 136–148. (f) Fachinetti, G.; Floriani, C.; Roselli, A.; Pucci, S. *J. Chem. Soc., Chem. Commun.* **1978**, 269–270. (g) Gell, K. I.; Schwartz, J. *J. Organomet. Chem.* **1978**, *162*, C11–C15. (h) Huffman, J. C.; Stone, J. G.; Krusell, W. C.; Caulton, K. G. *J. Am. Chem. Soc.* **1977**, *99*, 5829–5830. (i) Shoer, L. I.; Schwartz, J. *J. Am. Chem. Soc.* **1977**, *99*, 5831–5832.

(6) (a) Fagan, P. J.; Manriquez, J. M.; Marks, T. J. In "Organometallics of the f Elements"; Marks, T. J., Fischer, R. D., Eds.; D. Reidel Publishing Co.: Dordrecht, Holland, 1979; Chapter 4. (b) Marks, T. J.; Manriquez, J. M.; Fagan, P. J.; Day, V. W.; Day, C. S.; Vollmer, S. H. *ACS Symp. Ser.* **1980**, *131*, 1–29. (c) Marks, T. J. *Prog. Inorg. Chem.* **1979**, *25*, 224–383.

(7) (a) Fagan, P. J.; Manriquez, J. M.; Marks, T. J.; Day, V. W.; Vollmer, S. H.; Day, C. S. *J. Am. Chem. Soc.* **1980**, *102*, 5393–5396. (b) Manriquez, J. M.; Fagan, P. J.; Marks, T. J.; Day, C. S.; Day, V. W. *J. Am. Chem. Soc.* **1978**, *10*, 7112–7114. (c) Fagan, P. J.; Maatta, E. A.; Marks, T. J. *ACS Symp. Ser.*, in press.

(8) (a) Kroeker, R. M.; Kaska, W. C.; Hansma, K. *J. Catal.* **1980**, *61*, 87–95. (b) King, D. L. *Ibid.* **1980**, *61*, 77–86. (c) Krebs, H. J.; Bonzel, H. P. *Surf. Sci.* **1979**, *88*, 269–283. (d) Bioloen, P.; Helle, J. N.; Sachtler, W. H. M. *J. Catal.* **1979**, *58*, 95–107. (e) Dwyer, D. J.; Somorjai, G. A. *Ibid.* **1979**, *56*, 249–257. (f) *Ibid.* **1978**, *52*, 291–301 and footnote 9 therein. (g) Sexton, B. A.; Somorjai, G. A. *J. Catal.* **1977**, *46*, 167–188.

(9) (a) Connor, J. A. *Top. Curr. Chem.* **1977**, *71*, 71–110. (b) Kochi, J. K. "Organometallic Mechanisms and Catalysis"; Academic Press: New York, 1978; Chapter 11. (c) As an example, mean bond dissociation energies for ZrR_4 compounds vary from 54 (R = $CH_2C(CH_3)_3$) to 74 (R = CH_3) to 82 (R = $N(C_2H_5)_2$) to 103 (R = Cl) to 106 (R = O(i-C_3H_7)) kcal/mol.[9a]

(10) (a) Huheey, J. E. "Inorganic Chemistry", 2nd ed.; Harper and Row: New York, 1978; Appendix F. (b) Benson, S. W. "Thermochemical Kinetics", 2nd Ed.; Wiley-Interscience: New York, 1976; pp 72, 309.

(11) (a) At present there is a paucity of reliable bond energy data for organometallic hydrides. Those data which do exist[9,11b] and the instability of many metal hydrocarbyls with respect to β-hydride elimination argue that metal–carbon σ bonds are generally less stable than metal–hydrogen bonds. (b) Calado, J. G. C.; Dias, A. R.; Martinho, J. A.; Ribeiro da Silva, M. A. V. *J. Organomet. Chem.* **1979**, *174*, 77–80.

(12) (a) Collman, J. P.; Winter, S. R. *J. Am. Chem. Soc.* **1973**, *95*, 4089–4090. (b) Casey, C. P.; Neumann, S. M. *Ibid.* **1976**, *98*, 5395–5396. (c) Winter, S. R.; Cornett, G. W.; Thompson, E. A. *J. Organomet. Chem.* **1977**, *133*, 339–346.

(13) (a) Casey, C. P.; Neumann, S. M. *J. Am. Chem. Soc.* **1978**, *100*, 2544–2545. (b) Casey, C. P.; Andrews, M. A.; McAlister, D. R. *Ibid.* **1979**, *101*, 3371–3373. (c) Gladysz, J. A.; Selover, J. C.; Strouse, C. E. *Ibid.* **1978**, *100*, 6766–6768.

(14) This estimation is based upon the data in ref 9c and the general observation that trends in actinide(IV)–ligand bond energies closely parallel trends in Zr(IV)–ligand bond energies.[10a]

(15) For data illustrating the high affinity of f element and early transition-metal ions for oxygenated ligands, see ref 9 and the following: (a) Navrotsky, A. *Int. Rev. Sci.: Inorg. Chem., Ser. Two* **1975**, *5*, Chapter 2. (b) Keller, C. "The Chemistry of the Transuranium Elements"; Verlag Chemie: Weinheim/Bergstr., 1971; pp 151–152.

(16) (a) Fachinetti, G.; Floriani, C.; Stoeckli-Evans, H. *J. Chem. Soc. Dalton Trans.* **1977**, 2297–2302. (b) Fachinetti, G.; Fochi, G.; Floriani, C. *Ibid.* **1977**, 1946–1950. (c) In the zirconium compounds, the metal–oxygen distances are longer than the metal–carbon distances and ν_{CO} is ca. 85–160 cm^{-1} higher for nonconjugated R moieties.

(17) Fagan, P. J.; Manriquez, J. M.; Marks, T. J., manuscript in preparation.

To test this hypothesis, we have studied the carbonylation chemistry of two types of actinide–element bonds which are likely to be more resistant[9,11,14] to CO activation than the corresponding hydrocarbyls: dialkylamides (X = NR_2[18,20,21]) and hydrides (X = H).[19] In the present contribution we discuss the carbonylation chemistry of the former species, which are also of interest in their own right as highly unsaturated (judging from observed coordination numbers) precursors for new f-element chemistry.[18,20,21] We report here the first examples of CO insertion into a d- or f-element metal-to-dialkylamide bond, the informative properties of the resulting carbamoyl insertion products, and observations relevant to the course and stereochemistry of carbonylation in analogous actinide and possibly d-element hydrocarbyls. In particular, our chemical and structural results bear upon questions concerning the stereochemistry of CO insertion in bis(cyclopentadienyl)metal complexes (D or E)[4c] and the mechanism of

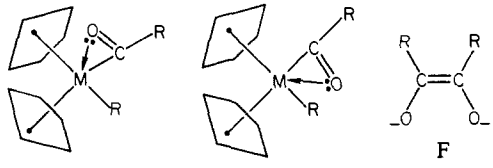

D E F

enediolate (F)[4a,6,7] formation from species such as B. In a later contribution we will deal with the rich carbonylation chemistry of organoactinide hydrides.[22]

Experimental Section

Physical and Analytical Measurements. ^1H NMR (60 MHz) and ^{13}C NMR (20 MHz) spectra were recorded on Perkin–Elmer R-20B and Varian CFT-20 spectrometers, respectively. Variable-temperature ^1H NMR spectra were recorded on a JEOL FX-90Q spectrometer. Chemical shifts are reported relative to internal $Si(CH_3)_4$. Samples were prepared either in a glovebox or on a high vacuum line. Deuterated aromatic solvents were dried over Na/K alloy, and CF_2Cl_2 was dried over freshly activated, degassed 4-Å Davison molecular sieves. All solvents were degassed by freeze–thaw cycles on a vacuum line.

Infrared spectra were recorded on Perkin-Elmer 267 or 283 spectrometers and were calibrated with polystyrene film. Samples were prepared in a glovebox as mulls by using previously dried and degassed Nujol or Fluorolube. Mulls were sandwiched between polished KBr plates contained in an airtight holder.

Elemental analyses were performed by Dornis and Kolbe Mikroanalytiches Laboratorium, West Germany.

Cryoscopic molecular weights were measured by using an apparatus similar to that described elsewhere[23] but modified for use on a vacuum line. In a typical procedure, an accurately weighed amount of benzene was condensed in vacuo into the molecular weight cell. Nitrogen (or argon) (1 atm) was introduced and the freezing point was recorded. The molecular weight cell was then brought into a nitrogen (or argon) filled glovebox, and a weighed amount of the complex to be measured was added. The freezing point of the solution was next recorded as before. The experimental error in molecular weights determined by this technique is estimated to be ±10%.

Materials and Methods. All manipulations were performed either in Schlenk-type glassware which was interfaced to a high vacuum (10^{-4}–10^{-5} torr) line or in a nitrogen (or argon) filled glovebox. Argon (Matheson, prepurified) and carbon monoxide (Matheson, C.P.) were purified further by passage through a supported MnO oxygen removal column[24] and a Davison 4-Å molecular sieve column. Reactions with CO were performed in an enclosed volume on the vacuum line, and gas uptake was monitored with a mercury manometer. Stohler 90% enriched carbon monoxide was employed for ^{13}CO studies. Toluene, diethyl ether, and pentane (previously distilled from Na/K/benzophenone) were condensed and stored in vacuo in bulbs on the vacuum line.

The lithium salts $LiN(CH_3)_2$ and $LiN(C_2H_5)_2$ were prepared by metalating the amines $(CH_3)_2NH$ (Matheson, anhydrous) and $(C_2H_5)_2NH$ (Aldrich, dried over Na) with *n*-butyl lithium (Aldrich, 1.6 M in hexane) at low temperature (−78 °C) in pentane. The white salts were isolated by filtration, washed with pentane, and dried in vacuo. The complexes $M[\eta\text{-}(CH_3)_5C_5]_2Cl_2$ (M = Th, U) and $U[\eta\text{-}(CH_3)_5C_5]_2(CH_3)_2$ were prepared by known procedures.[19a,25]

$Th[\eta\text{-}(CH_3)_5C_5]_2[N(C_2H_5)_2]Cl$ (1a). The synthesis of this colorless crystalline complex was similar to that described in detail below for $Th[\eta\text{-}(CH_3)_5C_5]_2[N(CH_3)_2]Cl$ with minor differences. In diethyl ether, 1.00 g (1.74 mmol) of $Th[\eta\text{-}(CH_3)_5C_5]_2Cl_2$ and 0.20 g (2.5 mmol) of $LiN(C_2H_5)_2$ were stirred for 12 h: yield 70%; IR data (Nujol mull) 1364 (s), 1350 (s), 1334 (m), 1276 (w), 1179 (s), 1142 (s), 1099 (w), 1050 (w), 1021 (m), 995 (s), 903 (w), 853 (s), 800 (w), 780 (m) cm^{-1}. Anal. Calcd for $C_{24}H_{40}NClTh$: C, 47.25; H, 6.61; N, 2.30; Cl, 5.81. Found: C, 47.34; H, 6.74; N, 2.35; Cl, 5.38.

$U[\eta\text{-}(CH_3)_5C_5]_2[N(C_2H_5)_2]Cl$ (1b). Dark red crystalline $U[\eta\text{-}(CH_3)_5C_5]_2[N(C_2H_5)_2]Cl$ was synthesized in (2.5 identical manner with that for $Th[\eta\text{-}(CH_3)_5C_5]_2[N(CH_3)_2]Cl$ (described below) by using 1.00 g (1.73 mmol) of $U[\eta\text{-}(CH_3)_5C_5]_2Cl_2$ and 0.20 g (2.5 mmol) of $LiN(C_2H_5)_2$: yield 70%; IR data (Nujol mull) 1364 (s), 1349 (s), 1334 (m), 1275 (w), 1176 (s), 1139 (s), 1095 (w), 1049 (w), 1020 (m), 995 (s), 903 (w), 855 (s), 802 (w), 780 (m) cm^{-1}. Anal. Calcd for $C_{24}H_{40}NClU$: C, 46.79; H, 6.54; N, 2.27; Cl, 5.76. Found: C, 46.70; H, 6.44; N, 2.35; Cl, 5.82.

$Th[\eta\text{-}(CH_3)_5C_5]_2[N(CH_3)_2]Cl$ (2a). A 50-mL round-bottomed flask was charged with 1.00 g (1.74 mmol) of $Th[\eta\text{-}(CH_3)_5C_5]_2Cl_2$ and 0.09 g (1.8 mmol) of $LiN(CH_3)_2$. On a vacuum line, diethyl ether (15 mL) was condensed into the flask. The reaction mixture was stirred at room temperature for 2.5 h. Solvent was next removed in vacuo. Toluene (10 mL) was condensed into the flask, and the solution was filtered into a 25-mL round-bottomed flask. The residual solids and upper portion of the filtration apparatus were washed by Soxhlet extraction in vacuo by condensing some of the toluene (3 mL) from the filtrate into the upper portion of the filtration apparatus. This washing was combined with the filtrate which was then concentrated in vacuo to 1 mL. Pentane (10 mL) was condensed into the flask in vacuo, and the resulting solution was cooled to −78 °C. The white crystalline product was isolated by cold filtration and was dried in vacuo; yield 71%. Recrystallization of this complex may be carried out in a manner similar to the isolation procedure.

IR data (Nujol mull): 2762 (s), 1237 (s), 1135 (s), 1058 (m), 1019 (m), 917 (s), 802 (w) cm^{-1}. Anal. Calcd for $C_{22}H_{36}ClNTh$: C, 45.40; H, 6.23; N, 2.41; Cl, 6.09; mol wt, 582. Found: C, 45.36; H, 6.29; N, 2.53; Cl, 6.12; mol wt, 610.

$U[\eta\text{-}(CH_3)_5C_5]_2[N(CH_3)_2]Cl$ (2b). Dark red crystalline $U[\eta\text{-}(CH_3)_5C_5]_2[N(CH_3)_2]Cl$ was synthesized in a manner identical with that for $Th[\eta\text{-}(CH_3)_5C_5]_2[N(CH_3)_2]Cl$ (described above) by using 1.00 g (1.73 mmol) of $U[\eta\text{-}(CH_3)_5C_5]_2Cl_2$ and 0.09 g (1.8 mmol) of $LiN(CH_3)_2$: yield 74%; IR data (Nujol mull) 2762 (s), 1235 (s), 1139 (s), 1054 (m), 1019 (m), 917 (s), 802 (w) cm^{-1}. Anal. Calcd for $C_{22}H_{36}ClNU$: C, 44.94; H, 6.17; N, 2.38; Cl, 6.03; mol wt, 588. Found: C, 44.87; H, 6.20; N, 2.42; Cl, 6.12; mol wt, 620.

$Th[\eta\text{-}(CH_3)_5C_5]_2[N(CH_3)_2]_2$ (3a). A 50-mL round-bottomed flask was charged with 1.00 g (1.74 mmol) of $Th[\eta\text{-}(CH_3)_5C_5]_2Cl_2$ and 0.25 g (4.9 mmol) of $LiN(CH_3)_2$. Diethyl either (15 mL) was condensed into the flask in vacuo, and the reaction mixture was stirred at room temperature for 1.5 h. Solvent was removed in vacuo. Pentane (10 mL) was next

(18) For reviews of metal dialkylamide chemistry, see: Eller, P. G.; Bradley, D. C.; Hursthouse, M. B.; Meek, D. W. *Coord. Chem. Rev.* **1977**, *24*, 1–95. (b) Harris, D. H.; Lappert, M. F. *J. Organomet. Chem. Libr.* **1976**, *2*, 13–102. (c) Bradley, D. C. *Adv. Chem. Ser.* **1976**, *No. 140*, 266–272. (d) *Adv. Inorg. Chem. Radiochem.* **1972**, *15*, 259–322.

(19) (a) Manriquez, J. M.; Fagan, P. J.; Marks, T. J. *J. Am. Chem. Soc.* **1978**, *100*, 3939–3941. (b) Broach, R. W.; Schultz, A. J.; Williams, J. M.; Brown, G. M.; Manriquez, J. M.; Fagan, P. J.; Marks, T. J. *Science (Washington, D.C.)* **1979**, *203*, 172–174. (c) Fagan, P. J.; Maatta, E. A.; Marks, T. J., manuscript in preparation.

(20) For recent work on lanthanide dialkylamide complexes see: (a) Ghotra, J. S.; Hursthouse, M. B.; Welch, A. J. *J. Chem. Soc., Chem. Commun.* **1973**, 669–670. (b) Bradley, D. C.; Ghotra, J. S.; Hart, F. A. *J. Chem. Soc., Dalton Trans.* **1973**, 1021–1023. (c) Bradley, D. C.; Ghotra, J. S.; Hart, F. A.; Hursthouse, M. B.; Raithby, P. R. *Ibid.* **1977**, 1166–1172. (d) Andersen, R. A.; Templeton, D. H.; Zalkin, A. *Inorg. Chem.* **1978**, *17*, 2317–2319.

(21) For recent work on actinide dialkylamide complexes see: (a) Bradley, D. C.; Ghotra, J. S.; Hart, F. A. *Inorg. Nucl. Chem. Lett.* **1974**, 209–211. (b) Jamerson, J. D.; Takats, J. *J. Organomet. Chem.* **1974**, *78*, C23–C25. (c) Reynolds, J. G.; Zalkin, A.; Templeton, D. H.; Edelstein, N. M.; Templeton, L. K. *Inorg. Chem.* **1976**, *15*, 2498–2502. (d) Reynolds, J. G.; Zalkin, A.; Templeton, D. H.; Edelstein, N. M. *Ibid.* **1977**, *16*, 599–603. (e) *Ibid.* **1977**, *16*, 1090–1096. (f) *Ibid.* **1977**, *16*, 1859–1861. (g) Turner, H. W.; Andersen, R. A.; Zalkin, A.; Templeton, D. H. *Ibid.* **1979**, *18*, 1221–1224. (h) Andersen, R. A. *Ibid.* **1979**, *18*, 1507–1509. (i) Turner, H. W.; Simpson, S. J.; Andersen, R. A. *J. Am. Chem. Soc.* **1979**, *101*, 2782.

(22) Fagan, P. J.; Maatta, E. A.; Manriquez, J. M.; Marks, T. J., manuscript in preparation.

(23) Shriver, D. F. "The Manipulation of Air-Sensitive Compounds"; McGraw-Hill: New York, 1969; p 162.

(24) McIlwrick, C. R.; Phillips, C. S. G. *J. Phys. E* **1973**, *6*, 1208–1210.

(25) Fagan, P. J.; Manriquez, J. M.; Marks, T. J., manuscript in preparation.

Table I. Vibrational Spectroscopic Data for Organoactinide η^2-Carbamoyls[a]

complex	ν_{CO}	$(\nu_{^{13}CO})$, cm^{-1}	ν_{CN}	$(\nu_{^{13}CN})$, cm^{-1}
$Th[\eta\text{-}(CH_3)_5C_5]_2\{\eta^2\text{-}CO[N(CH_3)_2]\}Cl$ (6a)	1546	(1524)	1320	(1289)
$U[\eta\text{-}(CH_3)_5C_5]_2\{\eta^2\text{-}CO[N(CH_3)_2]\}Cl$ (6b)	1559	(1539)	1318	(1290)
$Th[\eta\text{-}(CH_3)_5C_5]_2\{\eta^2\text{-}CO[N(C_2H_5)_2]\}Cl$ (7a)	1516	(1495)	1298	(1280)
$U[\eta\text{-}(CH_3)_5C_5]_2\{\eta^2\text{-}CO[N(C_2H_5)_2]\}Cl$ (7b)	1537	(1516)	1325	(1305)
$Th[\eta\text{-}(CH_3)_5C_5]_2\{\eta^2\text{-}CO[N(CH_3)_2]\}N(CH_3)_2$ (8a)	1521		1326	
$U[\eta\text{-}(CH_3)_5C_5]_2\{\eta^2\text{-}CO[N(CH_3)_2]\}N(CH_3)_2$ (8b)	1521		1326	
$U[\eta\text{-}(CH_3)_5C_5]_2\{\eta^2\text{-}CO[N(C_2H_5)_2]\}N(C_2H_5)_2$ (9a)	1491		1322	
$Th[\eta\text{-}(CH_3)_5C_5]_2\{\eta^2\text{-}CO[N(CH_3)_2]\}_2$ (10a)	1523		1346	
$U[\eta\text{-}(CH_3)_5C_5]_2\{\eta^2\text{-}CO[N(CH_3)_2]\}_2$ (10b)	1529		1340	
$U[\eta\text{-}(CH_3)_5C_5]_2\{\eta^2\text{-}CO[N(C_2H_5)_2]\}_2$ (11a)	1499		1301	

[a] Recorded as Nujol mulls (spectra recorded as Fluorolube mulls were essentially identical).

condensed into the flask, and the solution was filtered. The remaining solids were washed by Soxhlet extraction in vacuo by condensing 5 mL of pentane from the filtrate into the upper portion of the filtration apparatus. This washing was combined with the filtrate which was then cooled to −78 °C. The colorless crystalline precipitate was isolated by cold filtration and was dried in vacuo; yield 64%. Recrystallization of this complex may be carried out in a manner similar to the procedure for isolation.

IR data (Nujol mull): 2762 (s), 1236 (s), 1139 (s), 1125 (sh, m), 1062 (m), 1020 (m), 928 (s), 919 (s), 802 (w) cm^{-1}. Anal. Calcd for $C_{24}H_{42}N_2Th$: C, 48.80; H, 7.17; N, 4.74; mol wt, 591. Found: C, 48.69; H, 7.14; N, 4.79; mol wt, 570.

$U[\eta\text{-}(CH_3)_5C_5]_2[N(CH_3)_2]_2$ (3b). Orange crystalline $U[\eta\text{-}(CH_3)_5C_5]_2[N(CH_3)_2]_2$ was synthesized in an identical manner with that for $Th[\eta\text{-}(CH_3)_5C_5]_2[N(CH_3)_2]_2$ (described above) by using 1.00 g (1.73 mmol) of $U[\eta\text{-}(CH_3)_5C_5]_2Cl_2$ and 0.25 g (4.9 mmol) of $LiN(CH_3)_2$: yield 60%; IR data 2762 (s), 1233 (s), 1138 (s), 1121 (sh, m), 1059 (m), 1020 (m), 927 (s), 918 (s), 803 (w) cm^{-1}. Anal. Calcd for $C_{24}H_{42}N_2U$: C, 48.31; H, 7.10; N, 4.70. Found: C, 48.34; H, 7.20; N, 4.78.

$U[\eta\text{-}(CH_3)_5C_5]_2[N(C_2H_5)_2]_2$ (4a). A 25-mL round-bottomed flask was charged with 1.55 g (2.88 mmol) of $U[\eta\text{-}(CH_3)_5C_5]_2(CH_3)_2$.[19a,25] Diethylamine (4–5 mL) was condensed into the flask in vacuo at −78 °C. The reaction mixture was allowed to warm to room temperature, and argon was introduced. The solution was warmed to 60 °C with an oil bath and was stirred for 1 h at this temperature. The solution was then cooled to room temperature, and gases and excess diethylamine were removed in vacuo. Pentane (8 mL) was condensed into the flask, and the solution was filtered. The upper portion of the filtration apparatus was washed twice by Soxhlet extraction by condensing 4 mL of pentane from the filtrate. These washings were combined with the filtrate which was cooled to −78 °C. The orange-brown crystalline precipitate was isolated by cold filtration and was dried in vacuo: yield 40%; IR data (Nujol mull) 1365 (s), 1351 (s), 1334 (m), 1278 (w), 1175 (s), 1150 (s), 1098 (w), 1040 (w), 1019 (m), 998 (s), 899 (w), 858 (s), 799 (m), 781 (m) cm^{-1}. Anal. Calcd for $C_{28}H_{50}N_2U$: C, 51.52; H, 7.72; N, 4.29. Found: C, 51.36; H, 7.96; N, 4.39.

$Th[\eta\text{-}(CH_3)_5C_5]_2[N(CH_3)_2]CH_3$ (5a). A 50-mL round bottomed flask with a stopcock/sidearm was charged with 1.24 g (2.13 mmol) of $Th[\eta\text{-}(CH_3)_5C_5]_2[N(CH_3)_2]Cl$. Diethyl ether (10 mL) was condensed into the flask, and an atmosphere of argon was introduced. The flask was then cooled to −78 °C. Under a flush of argon, 1.35 mL of $CH_3Li\cdot LiBr$ (Aldrich, 1.75 M in diethyl ether) was syringed into the flask through the stopcock. The reaction mixture was stirred for 5 min at −78 °C and was then allowed to warm to room temperature. After 50 min, diethyl ether was removed in vacuo, and pentane (4 mL) was condensed into the flask. After filtration, the upper portion of the filtration apparatus was washed by Soxhlet extraction in vacuo, and this washing was combined with the filtrate. The filtrate was cooled to −78 °C, and the white crystalline precipitate was isolated by cold filtration and was dried in vacuo; yield 75%. Recrystallization of this complex may be carried out in a manner similar to the isolation procedure.

IR data (Nujol mull): 2760 (s), 1236 (s), 1142 (s), 1121 (m), 1107 (s), 1060 (m), 1019 (m), 914 (s), 800 (w) cm^{-1}. Anal. Calcd for $C_{23}H_{39}NTh$: C, 49.19; H, 7.00; N, 2.49. Found: C, 49.15; H, 6.91; N, 2.58.

$Th[\eta\text{-}(CH_3)_5C_5]_2[\eta^2\text{-}CO[N(CH_3)_2]]Cl$ (6a). A 25-mL round bottomed flask was charged with 0.38 g (0.65 mmol) of $Th[\eta\text{-}(CH_3)_5C_5]_2[N(CH_3)_2]Cl$. Toluene (8 mL) was next condensed into the flask. An atmosphere (ca. 700mmHg) of carbon monoxide was introduced and the flask was heated in an oil bath maintained at 95–100 °C. After 2.5 h, the solution was allowed to cool to room temperature. Solvent and carbon monoxide were removed in vacuo. Pentane (5 mL) was then condensed into the flask, and the solution was filtered. The upper portion of the filtration apparatus was washed with 4 mL of pentane by Soxhlet extraction in vacuo, and this washing was combined with the filtrate. The filtrate was concentrated to ca. 3 mL and was cooled to 0 °C. The colorless crystalline precipitate was isolated by cold filtration and was dried in vacuo; yield 60%. Recrystallization of this complex may be carried out in a manner similar to the isolation procedure.

IR data (Nujol mull): 1546 (s), 1410 (s), 1321 (s), 1252 (m), 1130 (m), 1021 (m), 892 (w), 802 (w), 652 (s) cm^{-1}. Anal. Calcd for $C_{23}H_{36}NOClTh$: C, 45.28; H, 5.95; N, 2.30; Cl, 5.81. Found: C, 45.19; H, 6.01; N, 2.36; Cl, 5.93.

$U[\eta\text{-}(CH_3)_5C_5]_2[\eta^2\text{-}CO[N(CH_3)_2]]Cl$ (6b). Orange-yellow crystalline $U[\eta\text{-}(CH_3)_5C_5]_2[\eta^2\text{-}CO[N(CH_3)_2]]Cl$ was synthesized in an identical manner to that for $Th[\eta\text{-}(CH_3)_5C_5]_2[\eta^2\text{-}CO[N(CH_3)_2]]Cl$ (described above) by using 0.40 g (0.68 mmol) of $U[\eta\text{-}(CH_3)_5C_5]_2[N(CH_3)_2]Cl$: yield 62%; IR data (Nujol mull) 1559 (s), 1410 (s), 1319 (m), 1253 (m), 1128 (m), 1021 (m), 893 (w), 802 (w), 653 (s). Anal. Calcd for $C_{23}H_{36}NOClU$: C, 44.84; H, 5.89; N, 2.27; Cl, 5.76. Found: C, 44.93; H, 5.95; N, 2.40; Cl, 5.83.

$Th[\eta\text{-}(CH_3)_5C_5]_2[\eta^2\text{-}CO[N(C_2H_5)_2]]Cl$ (7a). The colorless crystalline complex $Th[\eta\text{-}(CH_3)_5C_5]_2[\eta^2\text{-}CO[N(C_2H_5)_2]]Cl$ was synthesized in a manner similar to that described above for $Th[\eta\text{-}(CH_3)_5C_5]_2[\eta^2\text{-}CO[N(CH_3)_2]]Cl$ by using 0.50 g (0.82 mmol) of $Th[\eta\text{-}(CH_3)_5C_5]_2[N(C_2H_5)_2]Cl$: yield 52%; IR data (Nujol mull) 1516 (s), 1298 (s), 1211 (m), 1137 (w), 1080 (m), 1062 (m), 1020 (m), 1005 (w), 940 (w), 841 (w), 800 (w), 780 (w), 641 (m) cm^{-1}. Anal. Calcd for $C_{24}H_{40}NOClTh$: C, 47.06; H, 6.32; N, 2.20; Cl, 5.56. Found: C, 47.33; H, 6.40; N, 2.24; Cl, 5.44.

$U[\eta\text{-}(CH_3)_5C_5]_2[\eta^2\text{-}CO[N(C_2H_5)_2]]Cl$ (7b). Orange-yellow crystalline $U[\eta\text{-}(CH_3)_5C_5]_2[\eta^2\text{-}CO[N(C_2H_5)_2]]Cl$ was synthesized in a manner similar to that described above for $Th[\eta\text{-}(CH_3)_5C_5]_2[\eta^2\text{-}CO[N(CH_3)_2]]Cl$ by using 0.50 g (0.81 mmol) of $U[\eta\text{-}(CH_3)_5C_5]_2[N(C_2H_5)_2]Cl$: yield 54%; IR data (Nujol mull) 1537 (s), 1325 (s), 1211 (m), 1139 (w), 1088 (m), 1065 (m), 1020 (m), 1008 (w), 940 (w), 842 (w), 801 (w), 780 (w), 643 (m) cm^{-1}. Anal. Calcd for $C_{25}H_{40}NOClU$: C, 46.62; H, 6.26; N, 2.17; Cl, 5.50. Found: C, 46.49; H, 6.65; N, 2.34; Cl, 5.79.

$U[\eta\text{-}(CH_3)_5C_5]_2[\eta^2\text{-}^{13}CO(NR_2)]Cl$ (M = Th, U; R = CH_3, C_2H_5). The complexes derived from ^{13}CO were synthesized in a 25-mL round-bottomed flask which was attached to an adaptor which was in turn connected to the vacuum line. The adaptor had an inlet which was connected to the ^{13}CO gas storage bulb. The reactions were carried out in an enclosed volume at 95–100 °C for ca. 2–3 h in toluene by using typically 0.50–0.80 g of the starting actinide amide. The gas was removed then via Toepler pump and retained. Each product was isolated by a procedure identical with the isolation of the analogous product derived from ^{12}CO as described in detail above. Spectroscopic data are compiled in Table I.

$Th[\eta\text{-}(CH_3)_5C_5]_2[\eta^2\text{-}CO[N(CH_3)_2]]N(CH_3)_2$ (8a). A 25-mL round-bottomed flask was charged with 0.43 g (0.73 mmol) of $Th[\eta\text{-}(CH_3)_5C_5]_2[N(CH_3)_2]_2$, and toluene (8 mL) was then condensed into the flask. The solution was cooled to 0 °C (ice bath), and CO (740mmHg) was introduced. After 1.5 h, CO uptake ceased, and the solution was stirred for 30 min more, whereupon CO and toluene were removed in vacuo. Pentane (2–3 mL) was then condensed into the flask and the solution was filtered. The upper part of the filtration apparatus was washed once with 2 mL of pentane from the filtrate by Soxhlet extraction in vacuo. This washing was combined with the filtrate which was then cooled to −78 °C. Crystallization of the product was initiated by scratching the solution interface with the magnetic stirring bar with the aid of an external magnet. The colorless crystalline precipitate was isolated by cold filtration and was dried in vacuo; yield 33%. Recrystallization of this complex may be carried out in a manner similar to the isolation procedure.

IR data (Nujol mull): 2752 (s), 1521 (s), 1404 (s), 1393 (s), 1326 (s), 1253 (m), 1236 (s), 1148 (s), 1124 (s), 1062 (w), 1020 (m), 929 (s), 889 (w), 801 (w), 659 (s) cm^{-1}. Anal. Calcd for $C_{25}H_{42}N_2OTh$: C,

48.54; H, 6.84; N, 4.53. Found: C, 48.50; H, 6.88; N, 4.62.

U[η-(CH$_3$)$_5$C$_5$]$_2$[η^2-CO[N(CH$_3$)$_2$]]N(CH$_3$)$_2$ (8b). Orange crystalline U[η-(CH$_3$)$_5$C$_5$]$_2$[η^2-CO[N(CH$_3$)$_2$]]N(CH$_3$)$_2$ was synthesized by a procedure identical with that described above for Th[η-(CH$_3$)$_5$C$_5$]$_2$[η^2-CO-[N(CH$_3$)$_2$]]N(CH$_3$)$_2$ by using 0.65 g (1.09 mmol) of U[η-(CH$_3$)$_5$C$_5$]$_2$-[N(CH$_3$)$_2$]$_2$. Uptake of CO ceased after 1.75 h, and the solution was stirred for another 15 min before removing CO and toluene in vacuo; yield 44%. IR data (Nujol mull) 2760 (s), 1521 (s), 1404 (s), 1393 (s), 1326 (s), 1254 (m), 1235 (s), 1150 (s), 1121 (s), 1060 (s), 1020 (m), 926 (s), 890 (w), 801 (w), 654 (s) cm^{-1}. Anal. Calcd for C$_{25}$H$_{42}$N$_2$OU: C, 48.07; H, 6.78; N, 4.48. Found: C, 48.05; H, 6.80; N, 4.60.

U[η-(CH$_3$)$_5$C$_5$]$_2$[η^2-CO[N(C$_2$H$_5$)$_2$]]N(C$_2$H$_5$)$_2$ (9a). A 25-mL round-bottomed flask was charged with 1.20 g (1.84 mmol) of U[η-(CH$_3$)$_5$C$_5$]$_2$[N(C$_2$H$_5$)$_2$]$_2$. Toluene (10 mL) was condensed into the flask in vacuo, and the resulting solution was cooled to 0 °C. An atmosphere of CO was introduced, and the solution was stirred for 8 h. Toluene and CO were then removed in vacuo. Pentane (5 mL) was next condensed into the flask, and the solution was filtered. All attempts to crystallize the complex at −78 °C were unsuccessful. Pentane was then removed in vacuo, leaving a glassy orange-brown product. From the ^{1}H NMR, the product is estimated to be >95% pure.

IR data (Nujol mull): 1491 (s), 1363 (s), 1352 (s), 1322 (s), 1261 (m), 1219 (m), 1175 (m), 1151 (m), 1130 (m), 1100 (w), 1079 (w), 1063 (w), 1020 (m), 999 (s), 941 (m), 858 (s), 792 (m), 780 (m) cm^{-1}.

Th[η-(CH$_3$)$_5$C$_5$]$_2$[η^2-CO[N(CH$_3$)$_2$]]$_2$ (10a). A 25-mL round-bottomed flask was charged with 0.52 g (0.88 mmol) of Th[η-(CH$_3$)$_5$C$_5$]$_2$[N-(CH$_3$)$_2$]$_2$. Toluene (6 mL) was condensed into the flask, and an atmosphere of CO (700mmHg) was introduced. The solution was next heated with an oil bath maintained at 60 °C. Uptake of CO ceased after 1.25 h. The solution was allowed to stir for 1 h more and then was cooled to room temperature. Toluene and CO were removed in vacuo. Pentane (4 mL) was condensed into the flask and the solution was filtered. The upper portion of the filtration apparatus was washed with ca. 2 mL of pentane by Soxhlet extraction in vacuo. This washing was combined with the filtrate which was concentrated then to 2 mL and cooled to −78 °C. The white crystalline precipitate was isolated by cold filtration and dried in vacuo. At this point, the product was contaminated with 10% (by ^{1}H NMR) of the complex Th[η-(CH$_3$)$_5$C$_5$]$_2$[η^2-CO[N(CH$_3$)$_2$]]N(CH$_3$)$_2$. Recrystallization of the product from cold (−78 °C) pentane was required to remove this impurity: yield 35%; IR data (Nujol mull) 1523 (s), 1403 (s), 1392 (s), 1346 (s), 1257 (s), 1124 (s), 1049 (w), 1021 (m), 889 (m), 802 (w), 660 (s) cm^{-1}. Anal. Calcd for C$_{26}$H$_{42}$N$_2$O$_2$Th: C, 48.29; H, 6.55; N, 4.33. Found: C, 48.36; H, 6.64; N, 4.41.

U[η-(CH$_3$)$_5$C$_5$]$_2$[η^2-CO[N(CH$_3$)$_2$]]$_2$ (10b). Emerald green prisms of the complex U[η-(CH$_3$)$_5$C$_5$]$_2$[η^2-CO[N(CH$_3$)$_2$]]$_2$ were synthesized and purified in a manner similar to that described above for Th[η-CH$_3$)$_5$C$_5$]$_2$-[η^2-CO[N(CH$_3$)$_2$]]$_2$ by using 0.55 g (0.92 mmol) of U[η-(CH$_3$)$_5$C$_5$]$_2$[N-(CH$_3$)$_2$]$_2$. Uptake of CO was observed for ca. 1.5 h at 60 °C, and the color of the solution changed from orange to green. After being stirred for 1 h more, the solution was allowed to cool to room temperature. Recrystallization from cold (−78 °C) pentane was required to remove the monocarbonylated complex U[η-(CH$_3$)$_5$C$_5$]$_2$[η^2-CO[N(CH$_3$)$_2$]]N(CH$_3$)$_2$, which contaminated the crude product to the extent of about 10% as determined by ^{1}H NMR: yield 32%; IR data (Nujol mull) 1529 (s), 1405 (s), 1393 (s), 1340 (s), 1257 (s), 1122 (s), 1049 (w), 1021 (m), 889 (m), 802 (w), 660 (s) cm^{-1}. Anal. Calcd for C$_{26}$H$_{42}$N$_2$O$_2$U: C, 47.85; H, 6.49; N, 4.48. Found: C, 47.90; H, 6.54; N, 4.40.

U[η-(CH$_3$)$_5$C$_5$]$_2$[η^2-CO[N(C$_2$H$_5$)$_2$]]$_2$ (11a). The emerald green crystalline complex U[η-(CH$_3$)$_5$C$_5$]$_2$[η^2-CO[N(C$_2$H$_5$)$_2$]]$_2$ was synthesized in a manner similar to that for U[η-(CH$_3$)$_5$C$_5$]$_2$[η^2-CO[N(CH$_3$)$_2$]]$_2$ (described above) by using 1.00 g (1.53 mmol) of U[η-(CH$_3$)$_5$C$_5$]$_2$[N-(C$_2$H$_5$)$_2$]$_2$. The product was isolated from ca. 5 mL of cold (−78 °C) pentane. Great difficulty was encountered in initiating crystallization. However, once initiated, a low yield (~20%) of this complex was obtained. Recrystallization was accomplished from cold (−78 °C) pentane.

IR data (Nujol mull): 1499 (s), 1301 (s), 1260 (m), 1218 (m), 1131 (s), 1101 (m), 1080 (m), 1062 (m), 1021 (m), 1001 (m), 939 (m), 840 (m), 801 (w), 783 (m), 647 (s) cm^{-1}. Anal. Calcd for C$_{30}$H$_{50}$N$_2$O$_2$U: C, 50.84; H, 7.11; N, 3.95. Found: C, 50.99; H, 7.89; N, 4.44.

Th[η-(CH$_3$)$_5$C$_5$]$_2$[η^2-CO(CH$_3$)]N(CH$_3$)$_2$ (12a). A 25-mL round-bottomed flask was charged with 0.80 g (1.42 mmol) of the complex Th-[η-(CH$_3$)$_5$C$_5$]$_2$[N(CH$_3$)$_2$]CH$_3$. Toluene (5 mL) was condensed into the flask. An atmosphere of CO was introduced, and the solution was stirred at room temperature. Uptake of CO continued for 22 min and the solution color changed to yellow. After another 5 min, CO and toluene were removed in vacuo. Pentane (2 mL) was condensed into the flask and the solution was filtered. After the upper portion of the filtration apparatus was washed by Soxhlet extraction in vacuo, the filtrate was cooled to −78 °C, precipitating the yellow product which was then isolated by cold filtration and was dried in vacuo; yield 48%. Recrystallization of this complex can be carried out in a manner similar to the isolation procedure.

IR data (Nujol mull): 2753 (s), 1483 (s), 1322 (m), 1233 (s), 1153 (s), 1103 (m), 1018 (m), 922 (s), 800 (w) cm^{-1}. Anal. Calcd for C$_{24}$H$_{39}$NOTh: C, 48.89; H, 6.67; N, 2.38. Found: C, 49.04; H, 6.76; N, 2.31.

X-ray Crystallographic Studies[26] of Th[η-(CH$_3$)$_5$C$_5$]$_2$[η^2-CO[N-(C$_2$H$_5$)$_2$]]Cl (7a) and U[η-(CH$_3$)$_5$C$_5$]$_2$[η^2-CO[N(CH$_3$)$_2$]]$_2$ (10b). Large, well-shaped single crystals of Th[η-(CH$_3$)$_5$C$_5$]$_2$[η^2-CON(C$_2$H$_5$)$_2$]$_2$Cl (**7a**) (obtained by allowing a saturated, hot toluene solution to stand at 25 °C) and U[η-(CH$_3$)$_5$C$_5$]$_2$[η^2-CO[N(CH$_3$)$_2$]]$_2$ (**10b**) (obtained by slow cooling of a saturated pentane solution to −78 °C) were suitable for X-ray diffraction studies. Space group and unit cell data for the two compounds are monoclinic of space group $P2_1/n$ (an alternate setting of $P2_1/c$—C_{2h}^5 (No. 14)[27]) with a = 9.097 (2) Å, b = 21.191 (4) Å, c = 14.031 (2) Å, β = 95.78 (2)°, and Z = 4 (d_{calcd} = 1.567 g cm^{-3} and μ_a(Mo Kα)[28] = 6.43 mm^{-1}) for **7a** and monoclinic of space group $P2_1/c$—C_{2h}^5 (No. 14)[27] with a = 9.277 (4) Å, b = 16.143 (5) Å, c = 18.977 (6) Å, β = 130.55 (3)°, and Z = 4 (d_{calcd} = 1.584 g cm^{-3} and μ_a(Mo Kα)[28] = 5.59 mm^{-1} for **10b**. Intensity measurements were made on a computer-controlled Syntex P1 autodiffractometer for both compounds by using 1° wide ω scans and graphite-monochromated Mo Kα radiation. The sample of **7a** was a nearly cube-shaped specimen ~0.55 mm on an edge while that of **10b** was a multifaceted tabloid having principal faces of the form 100, 012, 0$\bar{1}$2, 0$\bar{1}$0, and 01$\bar{1}$ with minimum and maximum dimensions of 0.24 and 0.66 mm, respectively. A total of 6219 (**7a**) and 6336 (**10b**) independent reflections having $2\theta < 55°$ (the equivalent of 1.0 limiting Cu Kα spheres) were measured for both compounds in concentric shells of increasing 2θ containing approximately 3100 reflections each. Scanning rates of 3°/min were employed with both compounds for reflections having $2\theta_{MoK\alpha} < 43°$ and 2°/min with reflections having $43° < 2\theta_{MoK\alpha} < 55°$. The scan for each reflection was between ω settings 0.50° above and below the calculated Kα (λ = 0.71073 Å) doublet value. Counts were accumulated for 19 equal (time) intervals during each scan, and those 13 contiguous intervals which had the highest single accumulated count at their midpoint were used to calculate the net intensity from scanning. Background counts for reflections of both compounds, each lasting for half the total time used for the net scan (13/19 of the total scan time), were measured at ω settings 1° above and below the calculated Kα doublet value for each reflection. The intensity data for both compounds were corrected for absorption before applying Lorentz and polarization corrections.

The metal atoms of both compounds were located from Patterson syntheses and the remaining nonhydrogen atoms from difference Fourier syntheses. The oxygen atom of **7a** was disordered between two sites in the lattice and was assigned appropriate occupancy factors in all structure factor calculations. Unit-weighted full-matrix least-squares refinement cycles which incorporated anisotropic thermal parameters for the U, Th, and Cl atoms and isotropic thermal parameters for the remaining nonhydrogen atoms gave R_1 (unweighted, based on F) values of 0.089 and 0.044 for those reflections of **7a** and **10b**, respectively, having $2\theta_{MoK\alpha} < 43°$ and $I > 3\sigma(I)$. All structure factor calculations for both compounds employed the atomic form factors compiled by Cromer and Mann[29] and an anomalous dispersion correction[30] to the scattering factor of the U, Th, and Cl atoms. A least-squares refinable extinction correction[31] of the form $1/(1 + gI_c)^{1/2}$ was employed for structure factors of both compounds. The final cycles of empirically weighted full-matrix least-squares refinement which employed anisotropic thermal parameters for all nonhydrogen atoms of 7a converged to values of 0.080 and 0.097 for R_1 and R_2 (weighted, based on F), respectively, for 3156 independent reflections having $2\theta_{MoK\alpha} < 55°$ and $I > 3\sigma(I)$.[26] Similar refinement cycles for **10b** gave R_1 = 0.036 and R_2 = 0.042 for 3689 independent reflections having $2\theta_{MoK\alpha} < 55°$ and $I > 3\sigma(I)$.[26]

The programs previously described[32] were used on an IBM 360/65 or IBM 370/158 computer for this work.

Results

Synthesis and Properties of Bis(pentamethylcyclopentadienyl) Actinide Dialkylamido Complexes. The majority of the dialkyl-

(26) See paragraph at end of paper regarding supplementary material.
(27) "International Tables for X-Ray Crystallography"; Kynoch Press: Birmingham, England, 1969; Vol. I, p 99.
(28) "International Tables for X-Ray Crystallography"; Kynoch Press: Birmingham, England, 1974; Vol. IV, pp 55–56.
(29) Cromer, D. T.; Mann, J. L. *Acta Crystallogr., Sect. A* **1968**, *A24*, 321–324.
(30) Cromer, D. T. *Acta Crystallogr.* **1965**, *18*, 17–23.
(31) Zachariasen, W. H. *Acta Crystallogr.* **1967**, *23*, 558–564.
(32) Ernst, R. D.; Kennelly, W. J.; Day, C. S.; Day, V. W.; Marks, T. J. *J. Am. Chem. Soc.* **1979**, *101*, 2656–2664.

Table II. Room-Temperature ^{1}H NMR Spectroscopic Data for Organoactinide Amide and η^2-Carbamoyl Complexes[a,b]

compd	^{1}H NMR
Th[η-$(CH_3)_5C_5$]$_2$[$N(C_2H_5)_2$]Cl (1a)	2.03 (30 H, s), 0.99 (6 H, t, J = 7 Hz), 2.12 (4 H, q, J = 7 Hz)
U[η-$(CH_3)_5C_5$]$_2$[$N(C_2H_5)_2$]Cl (1b)	4.95 (30 H, s), 8.09 (6 H, br s, lw ≈ 23 Hz), 24.2 (4 H, br s; lw ≈ 80 Hz)
Th[η-$(CH_3)_5C_5$]$_2$[$N(CH_3)_2$]Cl (2a)	2.00 (30 H, s), 2.67 (6 H, s)
U[η-$(CH_3)_5C_5$]$_2$[$N(CH_3)_2$]Cl (2b)	5.56 (30 H, s), 25.1 (6 H, br s, lw ≈ 80 Hz)
Th[η-$(CH_3)_5C_5$]$_2$[$N(CH_3)_2$]$_2$ (3a)	1.99 (30 H, s), 2.85 (12 H, s)
U[η-$(CH_3)_5C_5$]$_2$[$N(CH_3)_2$]$_2$ (3b)	5.04 (30 H, s), −10.1 (12 H, s)
U[η-$(CH_3)_5C_5$]$_2$[$N(C_2H_5)_2$]$_2$ (4a)	4.85 (30 H, s), −5.00 (8 H, q, J = 7 Hz), −7.35 (12 H, t, J = 7 Hz)
Th[η-$(CH_3)_5C_5$]$_2$[$N(CH_3)_2$]CH_3 (5a)	1.94 (30 H, s), 0.30 (3 H, s), 2.51 (6 H, s)
Th[η-$(CH_3)_5C_5$]$_2${η^2-CO[$N(CH_3)_2$]}Cl (6a)	2.03 (30 H, s), 2.57 (3 H, s), 2.72 (3 H, s)
U[η-$(CH_3)_5C_5$]$_2${η^2-CO[$N(CH_3)_2$]}Cl (6b)	1.08 (30 H, s), 7.36 (3 H, s), −9.97 (3 H, s)
Th[η-$(CH_3)_5C_5$]$_2${η^2-CO[$N(C_2H_5)_2$]}Cl (7a)	2.05 (30 H, s), 0.97 (3 H, t, J = 7 Hz), 0.89 (3 H, t, J = 7 Hz), 3.23 (2 H, q, J = 7 Hz), 3.17 (2 H, q, J = 7 Hz)
U[η-$(CH_3)_5C_5$]$_2${η^2-CO[$N(C_2H_5)_2$]}Cl (7b)	0.50 (30 H, s), 16.2 (2 H, q, J = 7 Hz), 9.84 (3 H, t, J = 7 Hz), −12.18 (3 H, t, J = 7 Hz), −16.0 (2 H, q, J = 7 Hz)
Th[η-$(CH_3)_5C_5$]$_2${η^2-CO[$N(CH_3)_2$]}$N(CH_3)_2$ (8a)	1.98 (30 H, s), 2.72 (3 H, s), 2.83 (3 H, s), 3.08 (6 H, s)
U[η-$(CH_3)_5C_5$]$_2${η^2-CO[$N(CH_3)_2$]}$N(CH_3)_2$ (8b)	−1.82 (30 H, s), −22.9 (3 H, s), 11.80 (3 H, s), 87.0 (6 H, s)
U[η-$(CH_3)_5C_5$]$_2${η^2-CO[$N(C_2H_5)_2$]}$N(C_2H_5)_2$ (9a)	−1.82 (30 H, s), 30.2 (6 H, br s, lw ≈ 40 Hz), 13.17 (4 H, br s, lw ≈ 22 Hz) 19.6 (2 H, slightly broadened q), −0.52 (3 H, slightly broadened t), −12.2 (3 H, t J = 7 Hz), −16.2 (2 H, q, J = Hz)
Th[η-$(CH_3)_5C_5$]$_2${η^2-CO[$N(CH_3)_2$]}$_2$ (10a)	2.02 (30 H, s), 2.76 (6 H, s), 2.88 (6 H, s)
U[η-$(CH_3)_5C_5$]$_2${η-CO[$N(CH_3)_2$]}$_2$ (10b)	−5.02 (30 H, s), 33.4 (6 H, s), −14.7 (6 H, br s, lw ≈ 80 Hz)
U[η-$(CH_3)_5C_5$]$_2${η^2-CO[$N(C_2H_5)_2$]}$_2$ (11a)	−5.20 (30 H, s), 46.6 (4 H, slightly broadened q, J = 7 Hz), 26.5 (6 H, slightly broadened t, J = 7 Hz) −13.8 (6 H, br s, lw ≈ 36 Hz), −26.6 (4 H, br s, lw ≈ 70 Hz)
Th[η-$C_5(CH_3)_5$]$_2$[η^2-$CO(CH_3)$]$N(CH_3)_2$ (12a)	1.87 (30 H, s), 2.62 (3 H, s), 3.11 (6 H, s)

[a] Recorded in C_6D_6 at 35 °C; chemical shifts are reported relative to internal Me_4Si in ppm. [b] s = singlet; t = triplet; q = quartet; lw = line width.

amido precursors used in this study were straightforwardly prepared by the metathesis reaction shown in eq 3. This methodology

$$M[\eta\text{-}(CH_3)_5C_5]_2Cl_2 + x LiNR_2 \xrightarrow[25\ °C]{\text{diethyl ether}} M[\eta\text{-}(CH_3)_5C_5]_2(NR_2)_xCl_{2-x} + x LiCl \quad (3)$$

1a, x = 1, M = Th, R = C_2H_5 (colorless needles)

1b, x = 1, M = U, R = C_2H_5 (red-orange needles)

2a, x = 1, M = Th, R = CH_3 (colorless needles)

2b, x = 2, M = U, R = CH_3 (red-orange needles)

3a, x = 2, M = Th, R = CH_3 (colorless needles)

3b, x = 2, M = U, R = CH_3 (orange needles)

is similar to that previously employed in actinide, lanthanide, and transition element dialkylamido chemistry.[18,20,21] The extremely air-sensitive new compounds were isolated by crystallization from cold pentane or toluene/pentane mixtures. All compounds are soluble in toluene at room temperature, whereas only **3a** and **3b** are appreciably soluble in pentane at room temperature. Isolated yields in eq 3 were in the range 60–75% with no special attempt being made to optimize conditions. Possibly as a consequence of steric crowding, it proved difficult to cleanly introduce *two* diethylamido ligands via the approach of eq 3. However, such a complex could be prepared by reacting an actinide dialkyl with neat diethylamine (eq 4). Although this reaction proceeds

$$U[\eta\text{-}(CH_3)_5C_5]_2(CH_3)_2 + 2(C_2H_5)_2NH \xrightarrow{60\ °C} \underset{\mathbf{4a}}{U[\eta\text{-}(CH_3)_5C_5]_2[N(C_2H_5)_2]_2} + 2CH_4 \quad (4)$$

quantitatively (as indicated by ^{1}H NMR spectroscopy), the high solubility of **4a** precluded isolation in yields greater than ca. 40%, even by crystallization from pentane at −78 °C. In order to closely compare the carbonylation chemistry of M–CH_3 and M–$N(CH_3)_2$ linkages, we also synthesized a mixed hydrocarbyl dialkylamide complex (eq 5).

$$Th[\eta\text{-}(CH_3)_5C_5]_2[N(CH_3)_2]Cl + CH_3Li \xrightarrow[-78\ °C]{\text{ether}} \underset{\mathbf{5a}\ \text{(colorless needles)}}{Th[\eta\text{-}(CH_3)_5C_5]_2[N(CH_3)_2]CH_3} + LiCl \quad (5)$$

The new M[η-$(CH_3)_5C_5$]$_2$(NR_2)Cl, Th[η-$(CH_3)_5C_5$]$_2$[$N(CH_3)_2$]CH_3, and M[η-$(CH_3)_5C_5$]$_2$(NR_2)$_2$ complexes were characterized by infrared and ^{1}H NMR spectroscopy, by elemental analysis, and, in several cases, by cryoscopy in benzene (see Experimental Section for details). The vibrational spectra exhibit transitions at ca. 1020 and 800 cm^{-1} which are characteristic of η-pentamethylcyclopentadienyl ligands.[4a,6,7] Other bands at ca. 2763, 1235, 1139, 1059, and 920 cm^{-1} in the spectra of **2a**, **2b**, **3a**, **3b**, and **5a** as well as bands at ca. 1364, 1349, 1178, 1142, 995, and 853 cm^{-1} in the spectra of **1a**, **1b**, and **4a** can be attributed to σ-bonded dimethylamido and diethylamido functionalities, respectively.[18,20,21] Proton NMR data for these compounds are given in Table II. As is typical of U(IV) organometallics,[33] all the uranium complexes exhibit substantial isotropic shifts and, as a consequence of the short $5f^2$ electron spin–lattice relaxation times, relatively narrow line widths. Although the *N*-alkyl resonances are magnetically equivalent at room temperature, the line widths of the ^{1}H transitions are in excess of what is normally observed for U(IV) complexes,[33] and it was evident that this broadening might be due to an exchange process.

Important information on the structures and structural dynamics of the M[η-$(CH_3)_5C_5$]$_2$(NR_2)$_x$Cl$_{2-x}$ molecules is provided by variable-temperature NMR studies. As can be seen for U[η-$(CH_3)_5C_5$]$_2$[$N(CH_3)_2$]Cl in Figure 1, the broadened N–CH_3 singlet collapses upon lowering the temperature, and at −64 °C, two nonequivalent methyl resonances in a 1:1 intensity ratio are observed at δ 38.2 and 8.35. Down to −90 °C, the two η-$(CH_3)_5C_5$ ligands remain magnetically equivalent. This result argues against schematic ground state structures G and H for **2b**[34a] and implicates

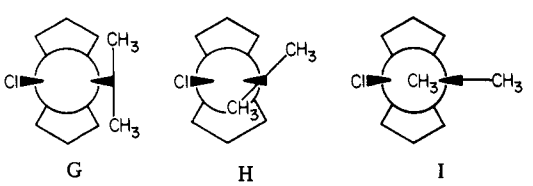

G H I

configuration I with coplanar Cl and $N(CH_3)_2$ functionalities.

(33) (a) Fischer, R. D. in ref 6a, Chapter 11. (b) Marks, T. J.; Seyam, A. M.; Kolb, J. R. *J. Am. Chem. Soc.* **1973**, *95*, 5529–5539.

(34) (a) In all mononuclear d- and f-element dialkylamide molecular structures reported to date,[18,20,21] the MNC_2 skeleton is essentially planar. (b) It is difficult at the present to assess the influence of the f orbitals in such matters. It should be noted, however, that an f orbital of appropriate symmetry (a_1) to overlap with the nitrogen lone pair in conformation I is available.

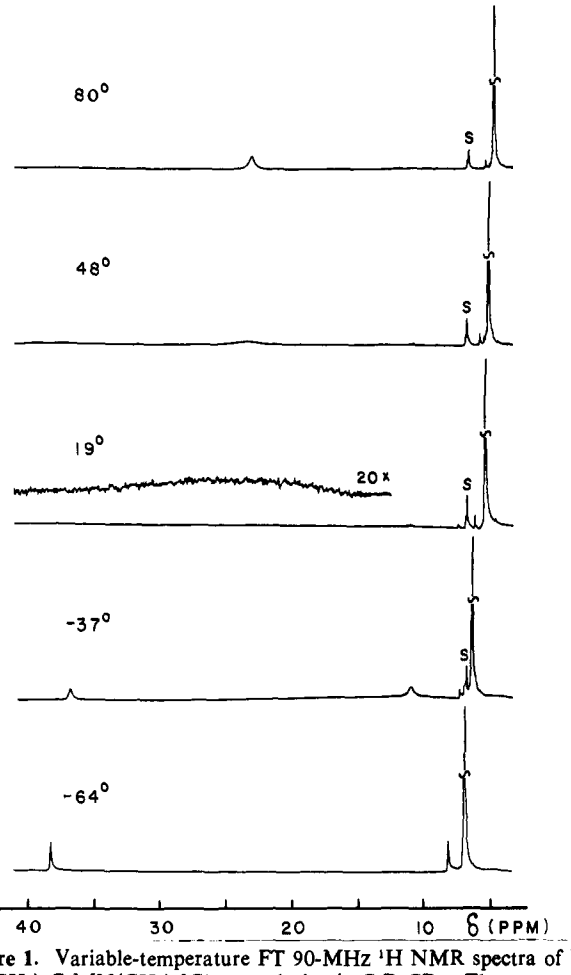

Figure 1. Variable-temperature FT 90-MHz ^1H NMR spectra of U-$[\eta\text{-}(CH_3)_5C_5]_2[N(CH_3)_2]Cl$ as a solution in $C_6D_5CD_3$. The resonance labeled S is due to toluene-d_7 and overlaps with the temperature-dependent $\eta\text{-}(CH_3)_5C_5$ resonance in the −64 °C spectrum.

Although structure G would allow better overlap between the nitrogen lone pair and the a_1 d orbital LUMO,[4c] molecular models suggest that unfavorable NCH_3–ring CH_3 nonbonded interactions are far greater in G than in I.[34b] The barrier to rotation about the U–N bond can be estimated from the standard coalescence point formalism[35] provided the frequency separation of the exchanging sites in the absence of exchange can be estimated at the coalescence temperature (21 °C). The isotropic shifts of the N–CH_3 resonances were found to obey an approximate Curie relationship (a plot of δ vs. $1/T$ is linear)[33,36] below the coalescence temperature, and an extrapolation of a least-squares fit to these data[37] yields $\Delta\delta$ = 1660 Hz and $\tau_c = 2.71 \times 10^{-4}$ s at this temperature. The $\Delta G^{\ddagger}$[38] for U–N bond rotation in U$[\eta\text{-}(CH_3)_5C_5]_2[N(CH_3)_2]Cl$ is thus estimated to be 12.4 ± 1.0 kcal/mol. This value compares favorably with barriers to analogous processes in transition-metal dialkylamides.[18]

Similar dynamic processes are also observed in the variable-temperature ^1H NMR spectra of U$[\eta\text{-}(CH_3)_5C_5]_2[N(CH_3)_2]_2$ as a solution in $C_6D_5CD_3$, with a slow exchange limit (−82 °C) spectrum consisting of two distinct N–CH_3 resonances at δ −15.8 and −34.6 in a 1:1 intensity ratio and a single $\eta\text{-}(CH_3)_5C_5$ signal. This result excludes schematic structures J and K but not structure L (of approximate C_2 symmetry) or M (of approximate C_{2v} symmetry). Employing the procedures described above, extrapolation of the N–CH_3 isotropic shifts to the spectral coalescence point (−44 °C)[39] and application of the standard relationships,[35] yields $\tau_c = 3.1 \times 10^{-4}$ s and $\Delta G^{\ddagger} = 9.6 \pm 1$ kcal/mol for rotation about the U–N bond.

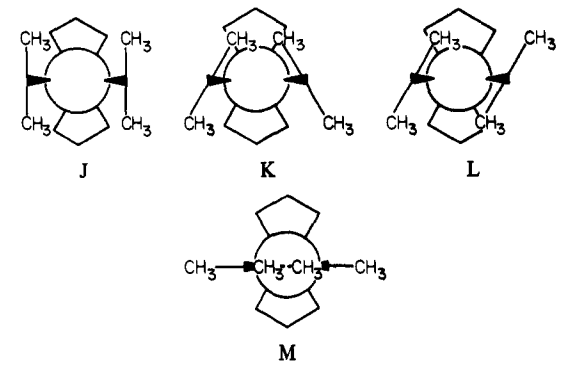

Attempts to obtain comparative molecular dynamic information for the diamagnetic thorium dialkylamides were not conclusive. Thus, Th$[\eta\text{-}(CH_3)_5C_5]_2[N(CH_3)_2]Cl$ (**2a**) exhibits an ^1H singlet N–CH_3 resonance down to −92 °C at 90 MHz with some broadening below −80 °C. It is not clear in this case whether the chemical shift difference between exchanging sites is too small to resolve, or whether it is not too small but that the barrier to rotation about the M–$N(CH_3)_2$ bond is substantially less for thorium than for uranium (possibly a consequence of the greater Th(IV) ionic radius[40] and reduced $N(CH_3)_2$–Cl interaction). Although the large chemical shift dispersion in the U(IV) system significantly alters the NMR time scale,[36a] it can be shown that for an exchanging site chemical shift difference of 10 Hz in the thorium system and identical $\Delta G^{\ddagger}$ values for **2a** and **2b**, the thorium coalescence point would still be accessible (calculated to be −35 °C).

Carbonylation of Chlorobis(pentamethylcyclopentadienyl)uranium and -thorium Dialkylamido Complexes. The chloro dialkylamido compounds **1a**, **1b**, **2a**, and **2b** react with CO at 95–100 °C (700mmHg) in toluene solution to yield carbamoyl[41] insertion products within 1.5–2.0 h (eq 6). No attempt was made to

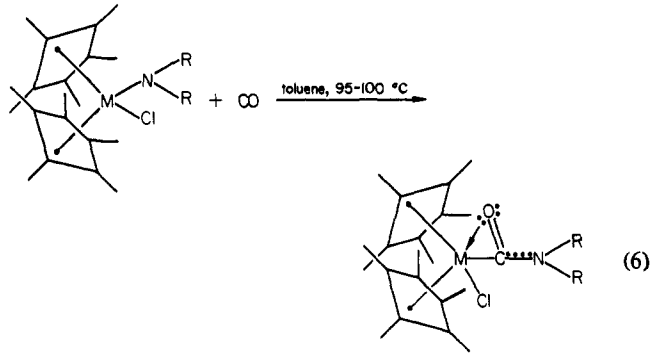

(6)

6a, M = Th, R = CH_3
6b, M = U, R = CH_3
7a, M = Th, R = C_2H_5
7b, M = U, R = C_2H_5

maximize the isolated yields, although CO uptake and sealed-tube ^1H NMR studies indicated the reaction to be essentially quantitative under these conditions. The new compounds were

(35) Binsch, G. In "Dynamic Nuclear Magnetic Resonance Spectroscopy"; Jackman, L. M., Cotton, F. A., Eds.; Academic Press: New York, 1975; pp 45–81.
(36) (a) Marks, T. J.; Kolb, J. R. *J. Am. Chem. Soc.* **1975**, *97*, 27–33. (b) Brunelli, M.; Lugli, G.; Giacometti, G. *J. Magn. Reson.* **1973**, *9*, 247–254. (c) von Ammon, R.; Fischer, R. D.; Kanellakopulos, B. *Chem. Ber.* **1972**, *105*, 45–62.
(37) $\delta_A = 2.80 \times 10^3(1/T) + 24.8$; $\delta_B = -5.41 \times 10^3(1/T) + 34.3$.
(38) $1/\tau = (kT/h)e^{-\Delta G^{\ddagger}/RT}$.
(39) $\delta_A = -5.83 \times 10^3(1/T) + 14.7$; $\delta_B = -8.86 \times 10^3(1/T) + 11.8$.
(40) (a) Shannon, R. D. *Acta Crystallogr., Sect. A* **1976**, *A32*, 751–767. Effective ionic radi for six-coordinate tetravalent ions: 0.94 Å (Th) and 0.89 Å (U). (b) Inspection of molecular models indicates that nonbonded interactions between *N*-alkyl groups and ring methyl groups will be severe in rotamers such as G and J.
(41) (a) Angelici, R. J. *Acc. Chem. Res.* **1972**, *5*, 335–341. (b) DellAmico, D. B.; Calderazzo, F.; Pelizzi, G. *Inorg. Chem.* **1979**, *18*, 1165–1168 and references therein. (c) Behrens, H.; Jungbauer, A. *Z. Naturforsch., B: Anorg. Chem., Org. Chem.* **1979**, *34B*, 1477–1486 and references therein. (d) Adams, R. D.; Chodosh, D. F.; Golembeski, N. M. *Inorg. Chem.* **1978**, *17*, 266–270.

characterized by standard techniques (see Experimental Section for details). The infrared spectra of **5** and **6** exhibit transitions in the 1510–1560 cm^{-1} and 1290–1325 cm^{-1} region which shift to lower energy upon ^{13}CO incorporation (Table I). The higher frequency transitions are assigned to modes which are predominantly C–O stretching in character. These are appreciably lower in energy than is generally observed for η^1 d element carbamoyl complexes (1565–1615 cm^{-1})[41] and suggest, by analogy to metal acyls,[4,6,7] η^2 coordination of the inserted CO functionality.[42] The bands at 1290–1350 cm^{-1} in the $M[\eta\text{-}(CH_3)_5C_5]_2[CONR_2]Cl$ compounds are assigned to modes with predominantly C–N stretching character.[42-44] Two trends in ν_{CO} are evident within the $M[(CH_3)_5C_5]_2[CONR_2]Cl$ series (Table I). First, for the same R functionality, the stretching frequencies for M = Th are always lower than those for M = U. This can be understood in terms of the greater oxygen affinity of thorium[15] (stabilization of resonance hybrid B); similar trends are observed for organoactinide η^2-acyls.[6,7] The second trend is the sensitivity of ν_{CO} to the identity of R: ν_{CO} for R = C_2H_5 is invariably lower than for R = CH_3. It seems unlikely that this ordering exclusively reflects differences in N–CH_3 and N–C_2H_5 inductive effects since such a shift is not observed in the ν_{CO} values for $HCON(CH_3)_2$ and $HCON(C_2H_5)_2$.[43] Rather, it is more likely in the present case that the shifts in ν_{CO} reflect distortions of the carbamoyl ligation due to greater intramolecular nonbonded repulsions for N–C_2H_5. A similar effect appears operative in $Zr(C_5H_5)_2\{\eta^2\text{-}CO[CH(Si(CH_3)_3)_2]\}Cl$.[5b] There is no indication in the vibrational data (Table I) that any of the above trends arise solely from variations in the ν_{CO}–ν_{CN} kinematic coupling. Substantial mixing of ν_{CO} and ν_{CN} is known to occur in free amides.[44]

Room-temperature ^1H NMR data for **5** and **6** are given in Table II. All of the U(IV) complexes exhibit large isotropic shifts and narrow line widths. The proton spectra of both thorium and uranium complexes exhibit magnetically nonequivalent alkyl functionalities, indicating that rotation about the C–N bond (eq 7) is slow on the time scale at room temperature. High-tem-

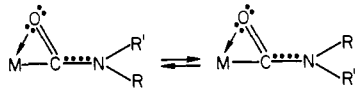

(7)

perature studies on **6a** reveal negligible broadening of the nonequivalent methyl resonances at temperatures up to 125 °C. With the assumption that any chemical exchange line broadening at this temperature is less than 2 Hz, it can be estimated from the standard kinetic/line shape relationships[35] that $\Delta G^{\ddagger}$ [38] for C–N rotation is greater than ca. 23 kcal/mol. Restricted rotation about the C–N bond has been observed in d element η^1-carbamoyl complexes, and, as in the case of organic amides, the barrier is attributed to multiple C–N bonding as shown in hybrid O.[41a] For

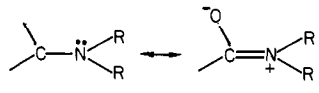

N O

transition-metal complexes, $\Delta G^{\ddagger}$ values depend upon the metal and ligands, with measured values ranging from ca. 14 to greater than 24 kcal/mol.[45] The present η^2 coordination is expected to further stabilize hybrid O, and the barrier to C–N rotation in the organoactinide carbamoyls may be extremely large. Further details of the molecular dynamics of the chloro carbamoyls will be discussed subsequent to the molecular structure.

The $^{13}C\{^1H\}$ NMR spectrum of $Th[\eta\text{-}(CH_3)_5C_5]_2[\eta^2\text{-}^{13}CON(C_2H_5)_2]Cl$ exhibits a strong signal at 248.5 ppm which is assigned to the carbamoyl carbon atom. The observed field position is considerably above the very low field, carbene-like value of 360.2 ppm found for $Th[\eta\text{-}(CH_3)_5C_5]_2[\eta^2\text{-}^{13}COCH_2C(CH_3)_3]Cl$,[7a] and suggests that coordinate π donation of nitrogen lone-pair electron density (hybrid O) may be an important factor in the bonding. This contention will be further supported by other data (vide infra). An analogous effect is observed for transition-metal "carbene" complexes.[46]

Solid-State Structure(s) of $Th[\eta\text{-}(CH_3)_5C_5]_2\{\eta^2\text{-}CO[N(C_2H_5)_2]\}Cl$ and Solution Molecular Dynamics. Final atomic coordinates and equivalent isotropic thermal parameters for nonhydrogen atoms of crystalline **7a** are presented in Table III; anisotropic thermal parameters for nonhydrogen atoms are given in Table IV.[26] The numbering scheme used to designate the atoms of **7a** is as follows. The atomic symbols for ring and methyl carbon atoms of the

Table III. Atomic Coordinates for Nonhydrogen Atoms in Crystalline $Th[\eta\text{-}(CH_3)_5C_5]_2\{\eta^2\text{-}CO[N(C_2H_5)_2]\}Cl$ (7a)[a]

atom type[b]	10^4x	10^4y	10^4z	equiv isotropic thermal parameter B,[c] Å
Th	3874.8 (7)	1253.6 (3)	2536.8 (4)	5.22
Cl	6367 (8)	946 (8)	3526 (7)	11.5
O'	5907 (31)	1945 (17)	2418 (21)	6.5
O	3044 (22)	2128 (9)	1471 (13)	4.8
N	5076 (20)	2720 (7)	1351 (12)	6.4
C	4582 (26)	2214 (10)	1785 (14)	6.1
C_{11}	4138 (39)	3093 (16)	569 (26)	11.4
C_{12}	3725 (47)	3681 (17)	925 (29)	12.8
C_{21}	6648 (30)	2876 (15)	1541 (24)	9.6
C_{22}	6967 (48)	3280 (26)	2345 (34)	14.3
C_{pa_1}	2209 (44)	2114 (12)	3503 (24)	7.9
C_{pa_2}	1292 (33)	1625 (19)	3277 (19)	8.5
C_{pa_3}	1685 (34)	1102 (9)	3801 (22)	6.9
C_{pa_4}	2973 (34)	1253 (19)	4391 (16)	7.5
C_{pa_5}	3335 (34)	1899 (22)	4190 (27)	7.6
C_{pb_1}	4007 (23)	61 (9)	1744 (17)	6.3
C_{pb_2}	2631 (24)	296 (14)	1368 (20)	7.2
C_{pb_3}	2901 (43)	775 (13)	751 (15)	7.5
C_{pb_4}	4383 (52)	816 (14)	746 (23)	8.0
C_{pb_5}	5043 (26)	373 (15)	1335 (22)	7.5
C_{ma_1}	2236 (92)	2780 (18)	3258 (45)	13.8
C_{ma_2}	−139 (44)	1712 (34)	2653 (25)	13.6
C_{ma_3}	722 (60)	477 (20)	3746 (33)	11.9
C_{ma_4}	3711 (64)	799 (28)	5127 (22)	12.8
C_{ma_5}	4564 (48)	2212 (32)	4766 (35)	14.4
C_{mb_1}	4224 (48)	−476 (14)	2467 (24)	11.2
C_{mb_2}	1170 (43)	−39 (26)	1510 (33)	13.8
C_{mb_3}	1490 (65)	1122 (21)	212 (29)	14.2
C_{mb_4}	5088 (78)	1292 (17)	43 (31)	11.9
C_{mb_5}	6721 (38)	202 (23)	1461 (33)	12.5

[a] Figures in parentheses are the estimated standard deviations in the last significant digit. [b] Atoms are labeled in agreement with Figure 2. [c] The nonhydrogen atoms were modeled with anisotropic thermal parameters of the form $\exp[(\beta_{11}h^2 + \beta_{22}k^2 + \beta_{33}l^2 + 2\beta_{12}hk + 2\beta_{13}hl + 2\beta_{23}kl)]$, and this is the equivalent isotropic thermal parameter calculated from $B = 4[V^2\det(\beta_{ij})]^{1/3}$.

(42) (a) There is one reported example of a mononuclear η^2-carbamoyl $(Mo(NO)[\eta^2\text{-}CON(CH_3)_2](NCS)_4^-)$: Müller, A.; Ulrich, S.; Werner, E. *Inorg. Chim. Acta* **1979**, *32*, L65–66. For dinuclear dihaptocarbamoyls, see: (b) Szostak, R.; Strouse, C. E.; Kaesz, H. D. *J. Organomet. Chem.* **1980**, *191*, 243–260 $(HRu_3[\eta^2\text{-}CON(CH_3)_2](CO)_{10})$. (b) Petz, W.; Kruger, C.; Goddard, R. *Chem. Ber.* **1979**, *112*, 3413–3423 $([Fe(CO)_4[\eta^2\text{-}CON(CH_3)_2]]_2Ni)$. (c) Keller, E.; Trenkle, A.; Vahrenkamp, H. *Ibid.* **1977**, *110*, 441–448 $(Fe_2[\mu\text{-}As(CH_3)_2][\eta^2\text{-}CON(CH_3)_2](CO)_6)$.

(43) "Sadtler Standard Infrared Spectra", Sadtler Research Laboratories, Inc., Philadelphia, PA.

(44) (a) Bellamy, L. J. "The Infrared Spectra of Complex Molecules", 3rd ed.; Chapman and Hall: London, 1975; Chapter 12. (b) Kniseley, R. N.; Fassel, V. A.; Farquhar, E. L.; Grey, L. S. *Spectrochim. Acta* **1962**, *18*, 1217–1229. (c) Beer, M.; Kessler, H. B.; Sutherland, G. B. B. M. *J. Chem. Phys.* **1958**, *29*, 1097–1104. (d) Suzuki, I. *Bull. Chem. Soc. Jpn.* **1962**, *35*, 540–551, 1279–1286.

(45) Calculated from the standard coalescence equations[35] and data in ref 41 and the following: (a) Green, C. R.; Angelici, R. J. *Inorg. Chem.* **1972**, *11*, 2095–2101. (b) Jetz, W.; Angelici, R. J. *J. Am. Chem. Soc.* **1972**, *94*, 3799–3802.

(46) (a) Cotton, F. A.; Lukehart, C. M. *Prog. Inorg. Chem.* **1972**, *16*, 487–613. (b) Schrock, R. R. *Acc. Chem. Res.* **1979**, *12*, 98–104. (c) Chisholm, M. H.; Godleski, G. *Prog. Inorg. Chem.* **1976**, *20*, 299–436. (d) Such NMR chemical shift trends must, of course, be interpreted with caution: Evans, J.; Norton, J. R. *Inorg. Chem.* **1974**, *13*, 3042–3043.

Table V. Bond Lengths and Angles Subtended at the Metal Atoms in Crystalline Th[η-$(CH_3)_5C_5]_2$\{η^2-CO[$N(C_2H_5)_2$]}Cl (7a) and U[η-$(CH_3)_5C_5]_2$\{η^2-CO[$N(CH_3)_2$]}$_2$ (10b)[a]

	value					value			
	7a, M = Th		10b, M = U			7a, M = Th		10b, M = U	
type[b]	ligand a	ligand b	ligand a	ligand b	type[b]	ligand a	ligand b	ligand a	ligand b
					Bond Lengths, Å				
M–O[c]	2.460 (16)	2.383 (31)	2.370 (5)	2.342 (7)	M–C_g[d]	2.28	2.33	2.30	2.29
M–C	2.418 (20)		2.405 (8)	2.402 (9)	M–C_{p_1}	2.812 (25)	2.779 (19)	2.771 (8)	2.789 (8)
M–Cl	2.619 (8)				M–C_{p_2}	2.778 (23)	2.784 (19)	2.794 (11)	2.752 (8)
M–C_r[d]	2.54	2.53	2.50	2.51	M–C_{p_3}	2.816 (20)	2.767 (22)	2.807 (10)	2.770 (8)
					M–C_{p_4}	2.806 (20)	2.762 (24)	2.768 (9)	2.793 (8)
					M–C_{p_5}	2.783 (21)	2.801 (22)	2.720 (9)	2.797 (8)
					Bond Angles, Deg				
OMC	34.2 (7)	37.3 (7)	30.9 (2)	31.2 (3)	$C_{rx}MC_{gy}$[d,e]	99.5	106.8	101.9	103.2
O_xMO_y[e]	71.5 (8)		153.0 (2)		C_rMCl[d]	102.4	100.9		
C_xMC_y[e]			92.7 (3)		C_rMO[d]	93.1	108.9	95.3	95.5
OMCl	135.1 (6)	63.6 (8)			C_rMC	105.2	103.0	98.8	98.8
CMCl	100.9 (7)				$C_{rx}MO_y$[d,e]	111.7	93.7	93.4	95.1
$C_{rx}MC_{ry}$[d,e]	138.9		138.0		$C_{rx}MC_y$[d,e]			109.5	110.5
C_rMC_g[d,e]	109.5	98.7	97.3	97.4					

[a] Figures in parentheses following an individual entry are the estimated standard deviation in the last significant digit. [b] Atoms are labeled in agreement with Tables III and VIII and Figures 2 and 5. [c] The entry for 7a listed under ligand a refers to O and that under ligand b refers to O'. [d] C_r refers to the center of gravity for the five-membered rings of the pentamethylcyclopentadienyl ligands. C_g refers to the midpoint of the carbamoyl C–O bond. [e] When listed under ligand a, the subscript x refers to a and y to b; when listed under ligand b, x refers to b and y to a.

Table VI. Ligand Bond Lengths in Crystalline Th[η-$(CH_3)_5C_5]_2$\{η^2-CO[$N(C_2H_5)_2$]}Cl (7a) and U[η-$(CH_3)_5C_5]_2$\{η^2-CO[$N(CH_3)_2$]}$_2$ (10b)[a]

	7a		10b			7a		10b	
type[b]	ligand a	ligand b	ligand a	ligand b	type[b]	ligand a	ligand b	ligand a	ligand b
O–C[c]	1.44 (3)	1.53 (4)	1.273 (10)	1.276 (12)	C_{p_1}–C_{p_2}	1.35 (4)	1.40 (3)	1.41 (1)	1.42 (1)
C–N	1.34 (2)		1.321 (10)	1.344 (13)	C_{p_1}–C_{p_5}	1.41 (5)	1.33 (4)	1.43 (1)	1.39 (1)
N–C_{11}	1.54 (3)		1.495 (13)	1.503 (15)	C_{p_2}–C_{p_3}	1.36 (4)	1.37 (4)	1.41 (2)	1.42 (1)
N–C_{21}	1.47 (3)		1.460 (13)	1.455 (17)	C_{p_3}–C_{p_4}	1.40 (4)	1.35 (4)	1.40 (2)	1.42 (1)
					C_{p_4}–C_{p_5}	1.45 (5)	1.36 (4)	1.40 (1)	1.39 (1)
C_{11}–C_{12}	1.41 (5)				C_{p_1}–C_{m_1}	1.46 (4)	1.53 (4)	1.53 (2)	1.53 (1)
C_{21}–C_{22}	1.43 (5)				C_{p_2}–C_{m_2}	1.51 (4)	1.54 (4)	1.54 (2)	1.52 (1)
					C_{p_3}–C_{m_3}	1.59 (4)	1.60 (5)	1.55 (2)	1.52 (1)
					C_{p_4}–C_{m_4}	1.52 (4)	1.59 (4)	1.53 (2)	1.54 (1)
					C_{p_5}–C_{m_5}	1.47 (4)	1.56 (4)	1.52 (1)	1.56 (1)

[a] Figures in parentheses following an individual entry are the estimated standard deviation in the last significant digit. [b] Atoms are labeled in agreement with Tables III and VIII and Figures 2 and 5. [c] The entry for 7a listed under ligand a refers to O and that under ligand b refers to O'.

Table VII. Ligand Bond Angles in Crystalline Th[η-$(CH_3)_5C_5]_2$\{η^2-CO[$N(C_2H_5)_2$]}Cl (7a) and U[η-$(CH_3)_5C_5]_2$\{η^2-CO[$N(CH_3)_2$]}$_2$ (10b)[a]

	7a, M = Th		10b, M = U			7a, M = Th		10b, M = U	
type[b]	ligand a	ligand b	ligand a	ligand b	type[b]	ligand a	ligand b	ligand a	ligand b
MOC[c]	71.3 (10)	72.6 (14)	76.1 (4)	77.0 (5)	$C_{p_5}C_{p_1}C_{p_2}$	107.3 (27)	107.7 (24)	107.2 (10)	108.2 (8)
MCO[c]	74.5 (11)	70.1 (15)	73.0 (4)	71.8 (5)	$C_{p_2}C_{p_2}C_{p_3}$	112.4 (30)	107.0 (23)	108.3 (11)	107.2 (8)
MCN	175.1 (16)		166.8 (7)	168.6 (8)	$C_{p_2}C_{p_3}C_{p_4}$	106.8 (27)	107.1 (24)	108.1 (10)	107.5 (7)
OCN[c]	108.9 (18)	106.5 (20)	120.2 (8)	119.5 (9)	$C_{p_3}C_{p_4}C_{p_5}$	107.3 (23)	109.4 (23)	108. (11)	108.1 (8)
CNC_{11}	123.5 (21)		122.7 (8)	120.3 (11)	$C_{p_4}C_{p_5}C_{p_1}$	106.1 (21)	108.7 (24)	107.7 (10)	109.1 (8)
CNC_{12}	117.8 (20)		121.0 (8)	120.9 (10)	$C_{p_2}C_{p_1}C_{m_1}$	135.9 (53)	124.6 (27)	126.8 (11)	125.4 (10)
$C_{11}NC_{21}$	118.1 (22)		116.3 (8)	118.7 (10)	$C_{p_5}C_{p_1}C_{m_1}$	116.7 (50)	127.6 (27)	125.7 (10)	125.4 (10)
					$C_{p_1}C_{p_2}C_{m_2}$	121.2 (43)	122.4 (36)	123.4 (14)	128.0 (9)
$NC_{11}C_{12}$	110.7 (29)				$C_{p_3}C_{p_2}C_{m_2}$	125.4 (45)	129.5 (35)	127.8 (13)	124.4 (9)
$NC_{21}C_{22}$	113.4 (31)				$C_{p_2}C_{p_3}C_{m_3}$	123.0 (40)	117.0 (38)	126.3 (15)	125.9 (9)
					$C_{p_4}C_{p_3}C_{m_3}$	130.2 (36)	135.9 (39)	125.4 (15)	126.4 (9)
					$C_{p_3}C_{p_4}C_{m_4}$	122.7 (46)	120.6 (47)	124.6 (12)	124.5 (9)
					$C_{p_5}C_{p_4}C_{m_4}$	130.0 (47)	129.7 (46)	126.6 (12)	126.9 (10)
					$C_{p_4}C_{p_5}C_{m_5}$	119.9 (53)	126.8 (38)	126.1 (11)	125.6 (10)
					$C_{p_1}C_{p_5}C_{m_5}$	133.4 (52)	124.2 (36)	126.1 (10)	125.0 (9)

[a] Figures in parentheses following an individual entry are the estimated standard deviation in the last significant digit. [b] Atoms are labeled in agreement with Tables III and VIII and Figures 2 and 5. [c] The entry for 7a listed under ligand a refers to O and that under ligand b refers to O'.

pentamethylcyclopentadienyl ligands have a (first) literal subscript p or m, respectively, and a (third) numerical subscript to distinguish between similar atoms within the same ligand. Alkyl substituents on the carbamoyl ligands have two numerical subscripts: the first distinguishes between alkyl substituents and the second between carbon atoms within the same substituent. A (second) literal subscripted a or b is used to distinguish between η-$(CH_3)_5C_5$ ligands.

A perspective model which illustrates the numbering scheme for **7a** is shown in Figure 2; each nonhydrogen atom is represented

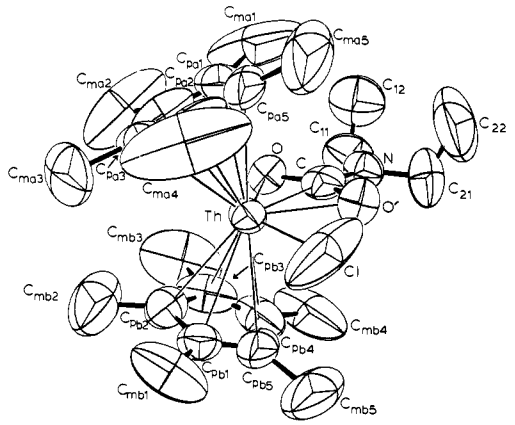

Figure 2. ORTEP drawing of the nonhydrogen atoms in the solid-state structure of $Th[\eta\text{-}(CH_3)_5C_5]_2\{\eta^2\text{-}CO[N(C_2H_5)_2]\}Cl$ (**7a**). All atoms are represented by thermal vibrational ellipsoids drawn to encompass 50% of the electron density. The numbering scheme is described in the text. The inserted CO has two possible orientations in the "equatorial girdle" with the oxygen atom disordered between two sites (O and O').

by an ellipsoid having the shape, orientation, and relative size consistent with the thermal parameters listed in Table IV.[26] Bond distances and angles subtended at the thorium atom are given with estimated standard deviations in Table V. Ligand bond lengths and angles are set out in Tables VI and VII, respectively.

The structural analysis reveals that crystals of **7a** are composed of discrete, mononuclear $Th[\eta\text{-}(CH_3)_5C_5]_2\{\eta^2\text{-}CO[N(C_2H_5)_2]\}Cl$ molecules (Figure 2) in which the Th(IV) ion adopts the familiar, pseudotetrahedral "bent sandwich" $M(\eta\text{-}C_5H_5)_2X_2$ configuration.[6,7,47] In **7a**, one X group is Cl^- and the other is an η^2-bonded *N,N*-diethylcarbamoyl ligand in which the oxygen atom (Figure 2) is disordered nearly equally between two sites (position O has an occupancy factor of 0.57 (2) and corresponds to isomer D; O' has an occupancy factor of 0.42 (3) and corresponds to isomer E). This disordering of the carbamoyl ligand is the result of both isomeric forms of **7a** being present in the crystal with nearly identical orientations of the carbamoyl nitrogen and ethyl functionalities. With the solid-state packing of $Th[\eta\text{-}(CH_3)_5C_5]_2\{\eta^2\text{-}CO(N(C_2H_5)_2]\}Cl$ undoubtedly dictated by the steric bulk of the $\eta\text{-}(CH_3)_5C_5$ ligands and the ethyl substituents of the carbamoyl moiety, the particular orientation of the inserted carbonyl group in the "equatorial girdle" should have only minor energetic consequences as long as nonbonded repulsions between O and Cl are not severe.

Despite the limitations in the accuracy of the metrical parameters for **7a** imposed by the disorder, it is possible to draw a number of meaningful conclusions. Moreover, it will be seen that the high precision analysis of a closely related bis(carbamoyl) compound (vide infra) supports and elaborates upon these conclusions. First, parameters describing the $M[\eta\text{-}(CH_3)_5C_5]_2$ portion of the coordination sphere differ little from non-carbamoyl bis(pentamethylcyclopentadienyl)thorium(IV) complexes. Thus, the (ring center of gravity)–Th–(ring center of gravity) angle (C_{ra}–Th–C_{rb}) of 138.9° compares favorably with that in $[\eta^2\text{-}COCH_2C(CH_3)_3]Cl$[6b,7a] (138°) and that in $\{Th[\eta\text{-}(CH_3)_5C_5]_2[\mu\text{-}CO(CH_2C(CH_3)_3)CO]Cl\}_2$ (134.9 (-, 12, 12, 2)°).[7a,48] Likewise, the average Th-C(ring) distance, 2.78 (4) Å, is comparable to average values in the above compounds of 2.788 (13) Å and 2.82 (2, 3, 5, 20) Å, respectively, and 2.83 (1) Å in $\{Th[\eta\text{-}(CH_3)_5C_5]_2H_2\}_2$.[7b] Each of the C_5 rings in **7a** are planar[49a] to within 0.017 Å, and the methyl substituent carbon atoms are displaced by as much as 0.28 Å out of the ring mean plane in the direction away from the metal ion. The average C–C distance of 1.38 (4, 3, 7, 10)[48] Å and C–CH_3 distance of 1.53 (1)[1,3,10] Å are typical values for $\eta\text{-}(CH_3)_5C_5$ bonding.[6,7,50] The orientations of the two pentamethylcyclopentadienyl rings about the local fivefold axes are interrelated due to interligand steric repulsion between methyl groups near the "equatorial girdle". Although several $C_{ma}\cdots C_{mb}$ contacts are significantly less (by as much as 0.61 Å) than the methyl group van der Waals diameter of 4.00 Å,[51] the orientations of the individual CH_3 groups about the threefold axes are no doubt such as to minimize interligand H···H and C···H contacts. Similar arguments can be made for other short intermolecular contacts in **7a** involving methyl groups.

The coordination of the diethylcarbamoyl moiety in **7a** is decidedly η^2 in each isomer. The least-squares mean plane of the points determining the "equatorial girdle" (atoms Th, Cl, O, O', C, and N are coplanar to within 0.06 Å)[49b] makes a dihedral angle of 90.4° with the plane[49b] defined by the metal and the two ring centers of gravity. The solid-state position determined for the inserted CO carbon atom probably corresponds to a point midway between half carbon atoms and introduces uncertainty in metrical parameters involving this atom. Nevertheless, it is interesting to note that the Th–C distance, 2.418 (20) Å, compares favorably with a value of 2.44 (3) Å in $Th[(CH_3)_5C_5]_2[\eta^2\text{-}COCH_2C(CH_3)_3]Cl$.[7a] Also, the Th–C–O angles, 74.5 (11) and 70.1 (15)°, are comparable to those in the above η^2-acyl, 73 (1)°. Such trends are in marked contrast to η^1-carbamoyls where M–C–O angles are in the range 122–124°.[41,52] The C–N distance of 1.34 (2)° in **7a** is not significantly different from that observed in η^1-carbamoyls[41,52] (typically 1.36 (10)–1.363 (10) Å) or in organic amides (1.366 (8)–1.380 (4) Å[53]). It is interesting to note that the Th–O distances in the two isomers of **7a** appear to be different, 2.460 (16) Å (D) and 2.383 (31) (E). The possibility that the long Th–O distance in D is electronically related to the short C–O distance (1.44 (3) Å) and that the short Th–O distance in E is furthermore electronically related to the long C–O' distance (1.53 (4) Å) is in accord with bonding expectations but is not, in the present case, conclusively supported by the certainty in the metrical data. Both C–O distances would appear to be greater than reported in transition-metal η^1-carbamoyls (1.214 (8)–1.25 (10) Å[41,52]) and organic amides (1.212 (3)–1.225 (3) Å[53]).

The solid-state structural results for **7a** raise questions of whether structures D and E are both significantly populated in solution at room temperature and whether rapid passage between them can take place.[4c,54] In Figure 3, variable-temperature ^1H NMR spectra of $U[\eta\text{-}(CH_3)_5C_5]_2\{\eta^2\text{-}CO[N(CH_3)_2]\}Cl$ (**6b**) as a solution in 1:1 $C_6D_5CD_3$–CF_2Cl_2 are presented. At −18 °C, singlets at δ −0.38 (30 H), 10.1 (3 H), and −14.1 (3 H) are observed which are assigned to the pentamethylcyclopentadienyl and the magnetically nonequivalent N–CH_3 resonances, respectively. Upon lowering the temperature, the $\eta\text{-}(CH_3)_5C_5$ resonance begins to broaden by ca. −70 °C, and in the limiting spectrum at −105 °C, this resonance has split into a doublet of unequal

(47) (a) Petersen, J. L.; Lichtenberger, C. L.; Fenske, R. F.; Dahl, L. F. *J. Am. Chem. Soc.* **1975**, *97*, 6433–6441 and references therein. (b) Prout, K.; Cameron, T. S.; Forder, R. A.; Critchley, S. R.; Denton, B.; Rees, R. V. *Acta Crystallogr. Sect. B* **1974**, *B30*, 2290–2304 and references therein.

(48) The first number in parentheses following an averaged value of a bond length or angle is the root-mean-square estimated standard deviation of an individual datum. The second and third numbers, when given, are the average and maximum deviations from the averaged value, respectively. The fourth number represents the number of individual measurements which are included in the average value.

(49) (a) Least-squares mean planes are defined by $-0.630X + 0.296Y + 0.7618Z = 3.87$ for atoms C_{pa1}–C_{pa5} and $-0.350X + 0.658Y - 0.752Z = 1.78$ for atoms C_{pb1}–C_{pb5}; X, Y, and Z are orthogonal coordinates along $\bar{a}$, $\bar{b}$, and $\bar{c}^*$. (b) Atoms Th, Cl, O, O', C, and N determine the plane described by the equation $-0.327X + 0.540Y + 0.776Z = 3.18$. Atoms C, O, N, C_{11}, and C_{21} determine the plane $-0.319X + 0.598Y + 0.735Z = 3.39$ and atoms C, O, N, C_{11}, and C_{21} $-0.324X + 0.613Y + 0.720Z = 3.43$.

(50) (a) Churchill, M. R.; Youngs, R. W. *Inorg. Chem.* **1979**, *18*, 1697–1702. (b) Churchill, M. R.; Julius, S. A. *Inorg. Chem.* **1979**, *18*, 2918–2920. (c) Freyberg, D. P.; Robbins, J. L.; Raymond, K. N.; Smart, J. C. *J. Am. Chem. Soc.* **1979**, *101*, 892–897.

(51) Pauling, L. "The Nature of the Chemical Bond", 3rd ed.; Cornell University Press: Ithaca, N.Y., 1960; p 260.

(52) Wagner, H.; Jungbauer, A.; Thiele, G.; Behrens, H. *Z. Naturforsch., B: Anorg. Chem., Org. Chem.* **1979**, *34B*, 1487–1490.

(53) It is important to compare gas phase data which are free of hydrogen-bonding effects: (a) Kitano, M.; Kuchitsu, K. *Bull. Chem. Soc. Jpn.* **1974**, *47*, 67–72 and references therein. (b) *Ibid.* **1974**, *47*, 631–634.

(54) (a) Erker, G.; Rosenfeldt, F. *Angew. Chem., Int. Ed. Engl.* **1978**, *17*, 605–606. (b) Erker, G.; Rosenfeldt, F. *J. Organomet. Chem.* **1980**, *188*, C1–C4.

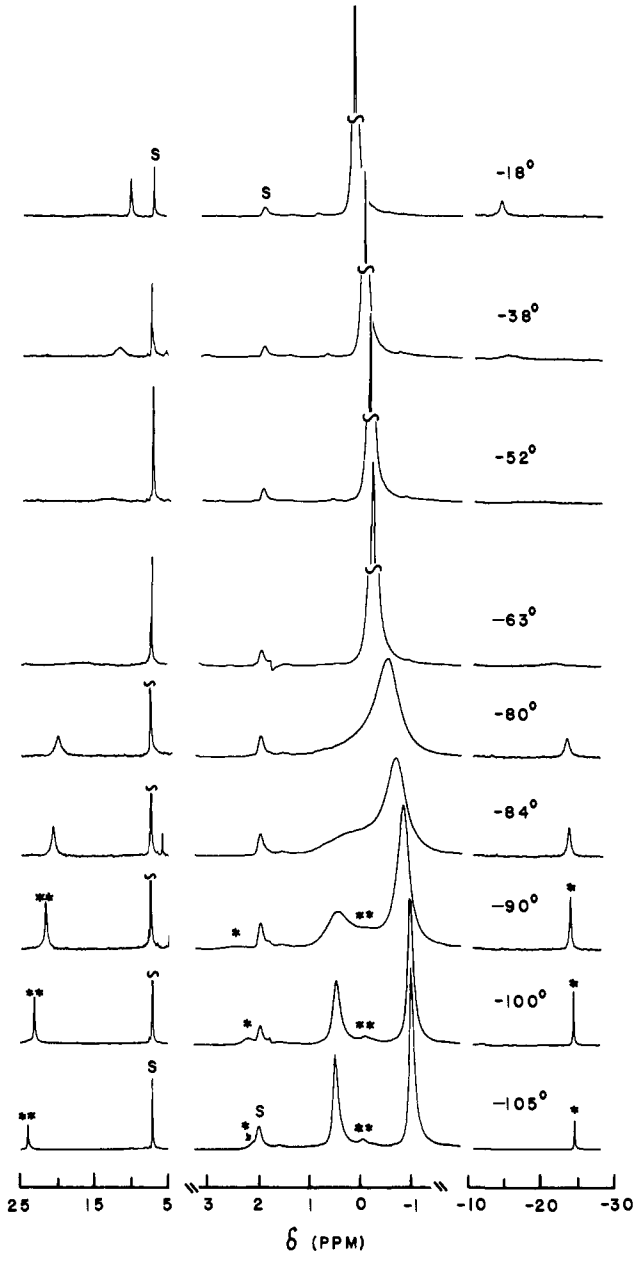

Figure 3. Variable-temperature FT 90-MHz ^1H NMR spectra of U-[η-$(CH_3)_5C_5$]$_2${η^2-CO[N$(CH_3)_2$]}Cl (**6b**) as a solution in 1:1 C_6D_5C-D_3–CF_2Cl_2. The resonances labeled asterisk and double asterisk indicate related pairs of exchanging N–CH_3 groups. The resonances labeled S (top and bottom spectrum) are due to toluene-d_7. The vertical scale may vary somewhat from spectrum to spectrum.

intensities at δ 0.62 (minor isomer) and −0.86 (major isomer) (K_{EQ}(−105 °C) = 1.71)). The two N–CH_3 resonances already begin to broaden at ca. −18 °C and eventually collapse at ca. −63 °C. In the limiting spectrum at −105 °C, two new pairs of N–CH_3 resonances which are assigned to methyl groups in the isomers D and E are observed at δ 23.7 and −24.4 (major isomer) and at δ 2.13 and 0.10 (minor isomer). All spectral changes are reversed upon raising the temperature and are independent of concentration. Analysis of these spectra was considerably complicated by partial overlap of resonances, the approximate Curie dependence ($\Delta\delta \approx 1/T$) of the resonance positions,[55] and the temperature dependence of the D ⇌ E equilibrium constant. Thus, the above assignments were verified by magnetization transfer experiments.[56] Strong irradiation at either of the signals indicated by an asterisk in Figure 3 at −88 °C results in a significant (ca. 50%) decrease in intensity of the other signal (relative to unaffected resonances) and indicates exchange between these two N–CH_3 sites. Similar experiments at −96 °C indicated the peaks labeled by a double asterisk in Figure 3 are also exchanging N–CH_3 sites. The dynamic process consistent with these observations is illustrated in eq 8. Importantly, the η^2-carbamoyl ligand reorients as a rigid unit, *without* permutation of nonequivalent R and R′ substituents.

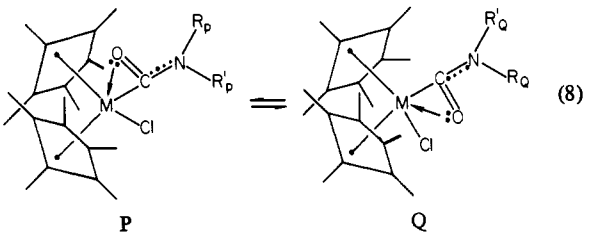

(8)

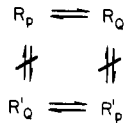

Application of the approximate kinetic line shape equations[35] to the η-$(CH_3)_5C_5$ resonances (after taking into account the Curie temperature dependence of the resonances[55]) at coalescence ($\Delta\delta$ = 118 Hz) yields $\tau = 2.6 \times 10^{-3}$ s and $\Delta G^{\ddagger} = 8.9 \pm 0.5$ kcal/mol at −80 °C.[57] A similar analysis of the two pairs (asterisk and double asterisk in Figure 3) of exchanging N–CH_3 sites yields $\Delta G^{\ddagger} = 9.1 \pm 0.5$ kcal/mol ($\Delta\nu^{**} = 1.44 \times 10^3$ Hz, $\tau^{**} = 2.1 \times 10^{-4}$ s at −52 °C) and $\Delta G^{\ddagger} = 9.2 \pm 0.5$ kcal/mol ($\Delta\nu^{*} = 2.26 \times 10^3$ Hz, $\tau^{*} = 1.3 \times 10^{-4}$ s at −44 °C). Clearly all sites are being permuted by the same process. From the temperature dependence of the relative intensities of the η-$(CH_3)_5C_5$ resonances below the slow exchange limit, approximate thermodynamic values for the D ⇌ E equilibrium can be calculated. Least-squares analysis of a plot of ln K_{EQ} vs. $1/T$ yields ln $K_{EQ} = -6.1 \times 10^2(1/T) + 4.2$, and thus, $\Delta H = 1.2 \pm 0.1$ kcal/mol, with $\Delta S = 8 \pm 1$ cal/(mol K).

It was next of interest to ascertain the kinetic and thermodynamic effects of bulkier substituents on the D ⇌ E (P ⇌ Q) equilibrium, and in Figure 4, variable-temperature ^1H NMR spectra for U[η-$(CH_3)_5C_5$]$_2${η^2-CO[N$(C_2H_5)_2$]}Cl (**7b**) as a solution in 1:1 $C_6D_5CD_3$–CF_2Cl_2 are illustrated. The changes are analogous to those observed for U[η-$(CH_3)_5C_5$]$_2${η^2-CO[N-$(CH_3)_2$]}Cl (**6b**) except that the presence of *N*-ethyl groups introduces greater spectral complexity, and the minor isomer is populated to a much lesser extent (K_{EQ} = 10 at −105 °C). This caused great difficulty in unambiguously locating the weak ethyl resonances associated with the minor isomer. Nevertheless, the similarity of the spectral changes suggests that an analogous D ⇌ E equilibrium occurs (eq 8) for **7b**. The limiting low-temperature spectrum obtained at −105 °C is assigned as follows: major isomer, δ −3.04 (η-$(CH_3)_5C_5$), 43.5 and −47.1 (ethyl CH_2's), and 26.7 and −26.4 (ethyl CH_3's); minor isomer, δ 0.20 (η-$(CH_3)_5C_5$). The kinetic line shape analysis was carried out by using standard procedures for exchanging systems with grossly nonequivalent populations.[58] Maximum broadening of the major isomer η-$(CH_3)_5C_5$ signal occurs at −70 °C. After the approximate

(55) For the complex U[η-$(CH_3)_5C_5$]$_2${η^2-CO[N$(CH_3)_2$]}Cl, the Curie temperature dependence of the exchanging resonances is given by the equations: $\delta = 5.50 \times 10^3(1/T) - 9.97$; $\delta = -9.02 \times 10^2(1/T) + 7.51$; $\delta = -98(1/T) + 1.2$; $\delta = 1.9 \times 10^2(1/T) - 1.0$; $\delta = -3.1 \times 10^2(1/T) + 0.99$; $\delta = -1.79 \times 10^3\ (1/T) - 1.40$.

(56) (a) McFarlane, W.; Rycroft, W. *Annu. Rep. NMR Spectrosc.* **1979**, *9*, 377–379. (b) Faller, J. W. In "Determination of Organic Structures by Physical Methods"; Nachod, F. C., Zuckerman, J. J., Eds.; Academic Press: New York, 1973; Vol. V, pp 75–106.

(57) At −80 °C, K_{EQ} is 2.7, a situation inbetween the graphical line shape analysis boundary conditions of equal populations[35] or grossly unequal populations.[58] Application of the modified Bloch equations for the coalescence point yields $\tau = 3.8 \times 10^{-3}$ s and $\Delta G^{\ddagger} = 9.0$ kcal/mol, while the Anet and Basus[58] equation for unequal populations and maximum line-broadening yields $\tau = 1.4 \times 10^{-3}$ s and $\Delta G^{\ddagger} = 8.6$ kcal/mol. Clearly these analyses give similar results; the values quoted in the text are the average.

(58) Anet, F. A. L.; Basus, F. J. *J. Magn. Reson.* **1978**, *32*, 339–343.

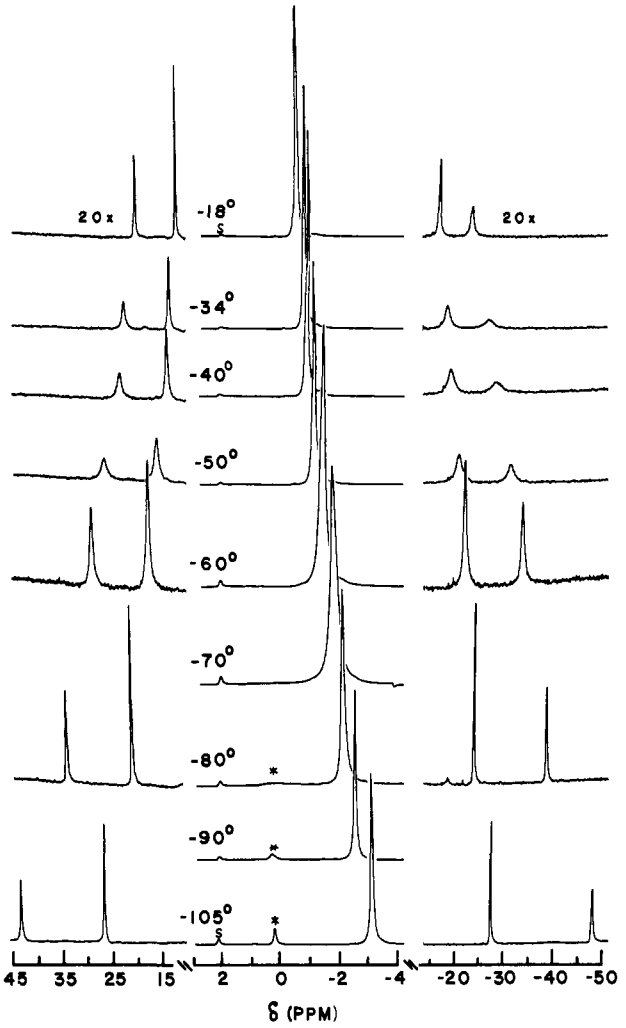

Figure 4. Variable-temperature FT 90-MHz ^1H NMR spectra of U-[η-$(CH_3)_5C_5]_2$[η^2-CO[$N(C_2H_5)_2$]]Cl (**7b**) as a solution in 1:1 C_6D_5C-D_3–CF_2Cl_2. The resonance labeled asterisk in the lower three spectra is the η-$(CH_3)_5C_5$ resonance of the minor isomer. The resonance labeled S (top and bottom spectra) is due to $C_6D_5CD_2H$. The vertical scale of the right and left portions of the spectra have been expanded 20× relative to the middle portion. The absolute vertical scale may vary somewhat from spectrum to spectrum.

Curie dependence of the chemical shifts was taken into account[59] the free energy of activation was determined to be $\Delta G^{\ddagger} = 8.9 \pm 0.5$ kcal/mol at −70 °C ($\Delta\nu$ = 200 Hz and $\tau = 8.0 \times 10^{-4}$ s at −70 °C). From a least-squares analysis of the temperature dependence of the equilibrium constant, the thermodynamic parameters $\Delta H = 0.8 \pm 0.3$ kcal/mol and $\Delta S = 9 \pm 3$ cal/(mol K) were determined.

Carbonylation of Bis(pentamethylcyclopentadienyl)uranium and -thorium Bis(dialkylamides). Despite the increased steric bulk about the actinide ion, the bis(dialkylamide) compounds **3a**, **3b**, and **4a** are more reactive toward CO than the chloro analogues. Thus, monocarbonylation is quantitatively complete within 2 h at 0 °C and 1 atm of CO (eq 9) as judged by gas uptake measurements and ^1H NMR spectroscopy. Isolated yields were substantially lower than 100% (see Experimental Section) and reflect the solubility characteristics of the materials under recrystallization conditions. The new compounds were characterized by standard methodology.

The monocarbonylated compounds **8a**, **8b**, and **9a** react with a second equivalent of CO in toluene under more forcing conditions

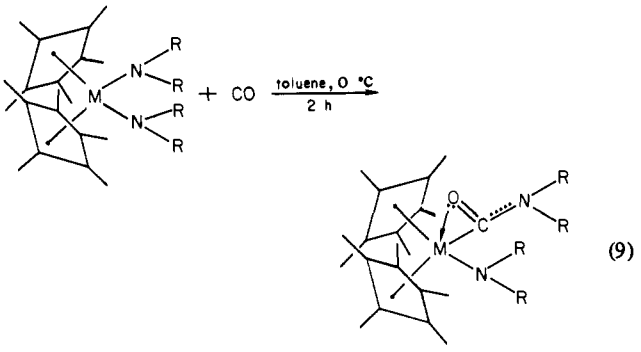

(9)

8a, M = Th, R = CH_3
8b, M = U, R = CH_3
9a, M = U, R = C_2H_5

(1 atm, 65 °C) to yield bis(carbamoyl) products (eq 10). Carbon

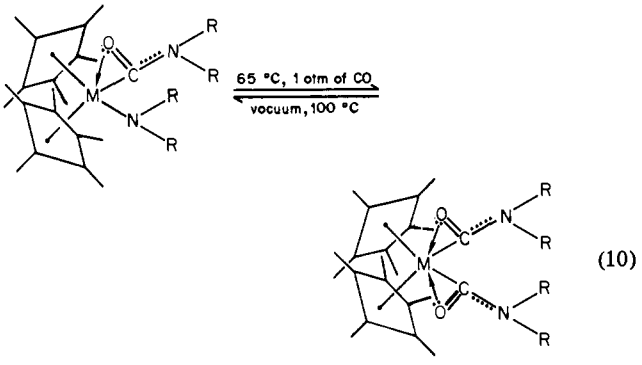

(10)

10a, M = Th, R = CH_3
10b, M = U, R = CH_3
11a, M = U, R = C_2H_5

monoxide uptake is complete in these systems within 1.5 h. Interestingly, when the solutions are maintained under vacuum at 100 °C, CO loss occurs and the bis(carbamoyls) revert to the monoinsertion products. This is the first case where CO extrusion has been observed in organoactinide carbonylation chemistry; in all other cases studied to date, carbon monoxide insertion is irreversible.[6,7] The bis(carbamoyls) were characterized by standard techniques (see Experimental Section). The low ν_{CO} values observed in the infrared spectra (Table I) indicate that both carbamoyl ligands are bound in a η^2 manner.

The infrared spectra in ν_{CO} and ν_{CN} region reveal several interesting trends. First, the C–O stretching frequencies of the M[η-$(CH_3)_5C_5]_2$[η^2-$CONR_2$]NR_2 compounds are lower than those of the M[η-$(CH_3)_5C_5]_2$[η^2-$CONR_2$]Cl analogues (Table I). This may indicate that chloride is a more effective π donor than dialkylamide in terms of quenching the actinide ion oxygen affinity. In the complexes M[η-$(CH_3)_5C_5]_2$[η^2-$CO(NR_2)$]$_2$, the ν_{CO} energies are comparable to those of the corresponding M[η-$(CH_3)_5C_5]_2$-[η^2-$CONR_2$]NR_2 derivatives, suggesting that the η^2-$CONR_2$ functionality is roughly comparable to NR_2 in reducing the carbonyl multiple bond character. Alternatively, the differences in vibrational frequencies may reflect distortions in structure caused by greater intramolecular steric congestion. Steric effects are likely significant since the sensitivity of ν_{CO} to R parallels that in the M[η-$(CH_3)C_5]_2$[η^2-$CO(NR_2)$]Cl series with ν_{CO} lower for R = C_2H_5. Thus, the complex U[η-$(CH_3)_5C_5]_2$[η^2-CO[N-$(C_2H_5)_2$]]$_2$, which is expected to have the most severe nonbonded repulsions, also has the lowest ν_{CO} of all the η^2 carbamoyls. The infrared data also evidence a modest sensitivity to M (ν_{CO} for M = Th being again lower than for M = U) in the complexes M[η-$(CH_3)_5C_5]_2$[η^2-$CONR_2$]$_2$. Interestingly, the sensitivity of ν_{CO} to M is considerably diminished in the M[η-$(CH_3)_5C_5]_2$-[η^2-$CONR_2$]NR_2 series, possibly reflecting an $-NR_2$ π-donor leveling effect.

Solid-State Structure of the Bis(carbamoyl) U[η-$(CH_3)_5C_5]_2$-{η^2-CO[$N(CH_3)_2$]}$_2$. Final atomic coordinates and equivalent isotropic thermal parameters for nonhydrogen atoms of crystalline

(59) For the complex U[η-$(CH_3)_5C_5]_2$[η^2-CO[$N(C_2H_5)_2$]]Cl, the Curie temperature dependence of the exchanging resonances is given by the following: $\delta = 1.12 \times 10^4(1/T) - 2.36$; $\delta = 7.05 \times 10^3(1/T) - 15.4$; $\delta = -2.6 \times 10^2(1/T) + 1.7$; $\delta = -3.83 \times 10^3(1/T) - 3.73$; $\delta = -1.12 \times 10^4(1/T) + 19.5$.

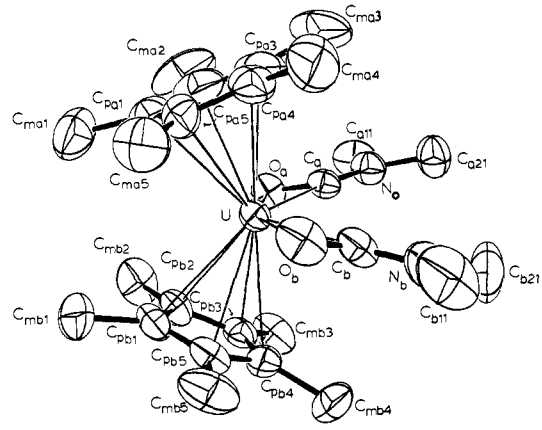

Figure 5. ORTEP drawing of the nonhydrogen atoms in the solid-state structure of $U[\eta\text{-}(CH_3)_5C_5]_2\{\eta^2\text{-}CO[N(CH_3)_2]\}_2$ (**10b**), oriented similarly to that for **7a** in Figure 2. All atoms are represented by thermal vibration ellipsoids drawn to encompass 50% of the electron density. The numbering scheme is described in the text.

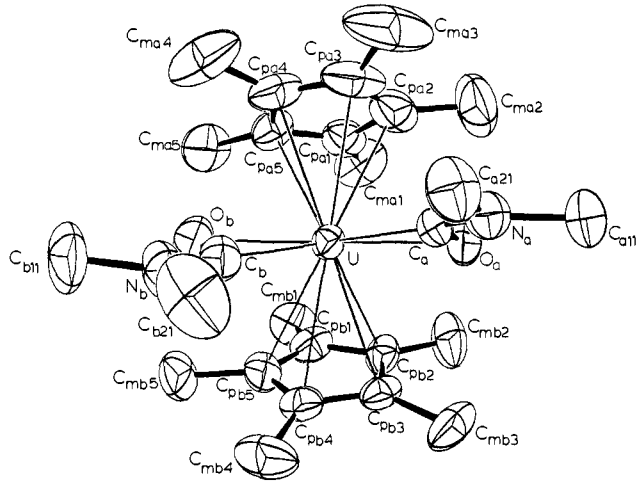

Figure 6. Second ORTEP drawing of the nonhydrogen atoms for **10b** viewed along the pseudo-C_2 axis of the molecule.

10b are compiled in Table VIII; anisotropic thermal parameters for nonhydrogen atoms are collected in Table IX.[26] The numbering scheme is the same as that employed for compound **7a** except that the two halves of **10b** related by a pseudo-C_2 axis passing through U and the midpoint of the vector between the carbamoyl C–O bonds (C_{ga} and C_{gb}) are distinguished from one another by a subscripted a or b.

Perspective models illustrating the numbering scheme for **10b** are presented in Figures 5 and 6; each nonhydrogen atom is described by an ellipsoid having the shape, orientation, and relative size consistent with the thermal parameters in Table IX. Bond distances and angles about the uranium ion are compiled in Table V along with estimated standard deviations. Metrical information for the ligands is given in Tables VI and VII. Unlike the disordered case of **7a**, the structural parameters for **10b** have been determined quite precisely (especially for an actinide).

Crystals of $U[\eta\text{-}(CH_3)_5C_5]_2[\eta^2\text{-}CO[N(CH_3)_2]]_2$ are composed of monomeric units with an $M[\eta\text{-}(CH_3)_5C_5]_2$ ligation structure closely resembling that of **7a** and previously mentioned mononuclear bis(pentamethylcyclopentadienyl) actinide complexes. The (ring center-of-gravity)–U–(ring-center-of-gravity) angle is a typical 138°. Any significant deviation of the average metal–C(cyclopentadienyl) distance in **10b** (2.788 (13) Å) from those of the aforementioned $Th[(CH_3)_5C_5]_2$ compounds is readily attributed to the 0.05 Å smaller ionic radius of six-coordinate U(IV).[40a] The average ring C–C and C–CH_3 bond distances in **10b** (1.41 (1, 1, 2, 10) Å[48] and 1.53 (1, 1, 3, 10) Å, respectively) are in good agreement with other $\eta\text{-}(CH_3)_5C_5$ determinations.[50] The C_5 atoms are coplanar to within 0.013 Å[60a] and the methyl carbon atoms are displaced from the plane in the direction away from the uranium ion by as much as 0.28 Å. The orientations of the $(CH_3)_5C_5$ rings about their respective fivefold axes as for **7a** appear to be dictated largely by methyl–methyl nonbonded interactions.

Table VIII. Atomic Coordinates for Nonhydrogen Atoms in Crystalline $U[\eta\text{-}(CH_3)_5C_5]_2\{\eta^2\text{-}CO[N(CH_3)_2]\}_2$ (10b)[a]

atom type[b]	10^4x	10^4y	10^4z	equiv isotropic thermal parameter B,[c] Å^2
U	2306.3 (3)	2462.9 (2)	−1302.2 (1)	2.94
O_a	1232 (6)	2494 (4)	−286 (3)	3.9
O_b	2445 (9)	2865 (4)	−2470 (4)	5.1
N_a	−431 (8)	3532 (5)	−481 (4)	4.2
N_b	300 (12)	3511 (5)	−3000 (4)	5.2
C_a	586 (9)	3081 (5)	−686 (4)	3.3
C_b	1157 (12)	3110 (5)	−2434 (5)	4.1
C_{a11}	−855 (13)	3399 (8)	224 (6)	5.4
C_{a21}	−1138 (12)	4230 (7)	−919 (6)	5.2
C_{b11}	872 (20)	3693 (8)	−3663 (6)	6.4
C_{b21}	−1174 (17)	3799 (9)	−2978 (8)	7.0
C_{pa1}	5183 (9)	2615 (7)	−477 (5)	4.8
C_{pa2}	4356 (12)	3129 (9)	−120 (7)	5.7
C_{pa3}	3864 (12)	3817 (8)	−565 (9)	5.6
C_{pa4}	4359 (11)	3728 (6)	−1200 (7)	5.0
C_{pa5}	5147 (10)	2985 (6)	−1164 (6)	4.3
C_{pb1}	2869 (10)	800 (5)	−1532 (6)	3.9
C_{pb2}	2018 (10)	812 (5)	−1003 (5)	3.6
C_{pb3}	564 (9)	1061 (5)	−1356 (5)	3.6
C_{pb4}	556 (10)	1214 (5)	−2091 (5)	3.8
C_{pb5}	1968 (11)	1057 (5)	−2187 (5)	3.9
C_{ma1}	6097 (14)	1855 (9)	−162 (8)	6.9
C_{ma2}	4238 (17)	2987 (13)	668 (7)	8.1
C_{ma3}	3039 (15)	4582 (9)	−362 (12)	7.4
C_{ma4}	4163 (17)	4378 (8)	−1801 (10)	7.8
C_{ma5}	5931 (12)	2663 (8)	−1728 (7)	6.1
C_{mb1}	4405 (11)	410 (8)	−1435 (7)	5.4
C_{mb2}	2470 (16)	515 (7)	−221 (6)	5.6
C_{mb3}	−767 (12)	1080 (6)	−1021 (7)	4.9
C_{mb4}	−840 (13)	1405 (8)	−2685 (7)	5.8
C_{mb5}	2435 (16)	1076 (7)	−2927 (6)	5.6

[a] Figures in parentheses are the estimated standard deviations in the last significant digit. [b] Atoms are labeled in agreement with Figure 5. [c] The nonhydrogen atoms were modeled with anisotropic thermal parameters of the form $\exp[(\beta_{11}h^2 + \beta_{22}k^2 + \beta_{33}l^2 + 2\beta_{12}hk + 2\beta_{13}hl + 2\beta_{23}kl)]$, and this is the equivalent isotropic thermal parameter calculated from $B = 4[V^2\det(\beta_{ij})]^{1/3}$.

The coordination of the η^2-carbamoyl ligands is the most interesting structural feature of **10b**. The average U–O bond distance, 2.356 (6, 14, 14, 2) Å, is significantly *shorter* than the average U–C distance, 2.404 (9, 2, 2, 2) Å, reflecting the high oxygen affinity of U(IV). Bearing in mind the ca. 0.05 Å greater ionic radius for Th(IV), these M–O vs. M–C parameters are comparable to those in **7a** (2.460 (16), 2.383 (31) Å vs. 2.418 (20) Å) and in $Th[\eta\text{-}(CH_3)_5C_5]_2[\eta^2\text{-}COCH_2C(CH_3)_3]Cl$ (2.37 (2) vs. 2.44 (2) Å); for comparison, a Th–O single bond distance is 2.154 (8) Å.[7b] The relative shortness of U–O vis-à-vis U–C stands in marked contrast to the only known mononuclear transition-metal η^2-carbamoyl, $Mo(NO)[\eta^2\text{-}CON(CH_3)_2](NCS)_4^-$, where Mo–O = 2.078 (6) Å and Mo–C = 2.029 (6) Å.[42a] The C–O bond length in **10b**, 1.275 (11, 2, 2, 2) Å, is significantly longer than in organic amides (1.212 (3)–1.225 (3) Å[53]) and probably longer than in most η^1-carbamoyl transition-metal complexes (1.214 (8)–1.251 (10) Å[41,52]); the distances are slightly shorter than in the molybdenum η^2-carbamoyl, 1.322 (8) Å. The average C–N distance in **10b**, 1.333 (14, 12, 12, 2) Å, is likely shorter than in organic amides (1.366 (8)–1.380 (4) Å[53]) and is slightly less than or

(60) (a) Least-squares mean planes are defined by $0.736X + 0.494Y + 0.417Z = 5.54$ for atoms C_{pa1}–C_{pa5} and $0.212X + 0.952Y + 0.220Z = 1.32$ for atoms C_{pb1}–C_{pb5}. (b) Least-squares mean planes are defined by $0.627X + 0.624Y + 0.466Z = 3.05$ for atoms C_a, O_a, N_a, X_{a11}, and C_{a21} and $0.297X + 0.868Y + 0.398Z = 3.20$ for atoms C_b, O_b, N_b, C_{b11}, and C_{b21}. (c) This plane is described by the equation $0.538X + 0.779Y + 0.322Z = 3.79$.

comparable to that in η^1-carbamoyls (1.336 (10)–1.363 (10) Å); the **10b** C–N distance appears to be longer than in the aforementioned molybdenum compound, 1.240 (10) Å. For comparison, typical C=O and C–O distances in organic compounds are 1.21 and 1.416 Å, respectively, and C=N and C–N distances are 1.24 and 1.474 Å, respectively.[61] The average M–C–O angle in **10b**, 72.4 (4, 5, 5, 2)°, compares favorably with those in **7a** (74.5 (11)° and 70.1 (15)°) and that in $Th[\eta\text{-}(CH_3)_5C_5]_2[\eta^2\text{-}COCH_2C(CH_3)_3]Cl$, 73 (1)°. The η^2-carbamoyl ligands in **10b** are planar to within 0.024 Å and their least-squares mean planes[60b] make angles of 13.2° and 15.4° with that determining the "equatorial girdle" (i.e., that defined by the uranium atom and the midpoints of the carbamoyl C–O bonds (C_{ga} and C_{gb})).[60c] As can be appreciated in Figure 6, the coordinated CO units of the planar η^2-$CON(CH_3)_2$ ligands are rotated out of the equatorial plane by 13.2 and 15.4°. This rotation appears to result from nonbonded repulsion between carbon atoms C_{a21} and C_{b21} of the planar carbamoyl groups. Even so, a short $C_{a21}\cdots C_{b21}$ contact of 3.96 (3) Å is observed. Both of these carbamoyl methyl groups are also involved in a short intramolecular contact with a ring methyl group ($C_{a21}\cdots C_{ma3}$ = 3.81 (3) Å and $C_{b21}\cdots C_{mb4}$ = 3.96 (3) Å).

Carbonylation of the Alkyl Dialkylamide $Th[\eta\text{-}(CH_3)_5C_5]_2[N(CH_3)_2]CH_3$. The relative reactivities of Th–CH_3 and Th–$N(CH_3)_2$ bonds with respect to migratory CO insertion were examined in an intramolecular competition experiment. As shown in eq 11,

$$Th[(CH_3)_5C_5]_2[N(CH_3)CH_3] \xrightarrow{CO} Th[\eta\text{-}(CH_3)_5C_5][\eta^2\text{-}CO(CH_3)]N(CH_3)_2 \quad (11)$$
12

insertion initially occurs into the metal–carbon σ bond to yield a η^2-acyl (**12**) with ν_{CO} = 1483 cm^{-1} (ν_{CO} = 1469 cm^{-1} in $Th[\eta\text{-}(CH_3)_5C_5]_2[\eta^2\text{-}COCH_2(CH_3)_3]Cl$). Efforts to introduce further CO units resulted in complex mixtures of inseparable products.

Thermal Properties of $U[\eta\text{-}(CH_3)_5C_5]_2\{\eta^2\text{-}CO[N(CH_3)_2]\}_2$. Heating the bis(carbamoyl) complex **10b** did not cleanly effect ring closure to an enediolate (eq 12). Reactions at 100 °C under

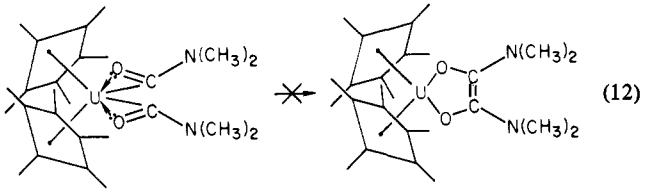

(12)

nitrogen resulted only in decarbonylation to produce the corresponding monocarbamoyl **8b**. Under a carbon monoxide atmosphere (1.5 atm) at 110 °C in toluene solution, an ill-defined, air-stable, brick-red microcrystalline precipitate formed after 24 h which was completely insoluble in all organic solvents. The supernatant solution contained mostly $U[\eta\text{-}(CH_3)_5C_5]_2\{\eta^2\text{-}CO[N(CH_3)_2]\}N(CH_3)_2$ as determined by ^1H NMR spectroscopy. The precipitate exhibited strong, broadened bands at 1510, 1380 (very broad), 1310, 1262, 1224, 1139, and 1055 cm^{-1} and weaker bands at 1020 (sh), 910, 782, 762, and 694 cm^{-1} in the infrared spectrum. Clearly, some other process occurs rather than simple enediolate formation. The solubility properties suggest an oligomeric product, and the infrared spectrum is not readily assigned to an enediolate ligand.[6,7]

Discussion

The results of this study demonstrate the first activation and migratory insertion of carbon monoxide into a d- or f-element metal–NR_2 bond. Such insertion reactions have been previously proposed[62] as components of a number of stoichiometric and catalytic carbonylation reactions but have never been unambiguously identified. In this case involving the bis(pentamethylcyclopentadienyl) actinide coordination environment, the reaction is facile (although not competitive with insertion into actinide–methyl bonds) and the reaction products are mono and bis(η^2-carbamoyl) complexes. Judging from the spectroscopic and metrical data, the strong metal–oxygen interaction plays a major role in the bonding and in driving the insertion reaction. It is likely that the ionic character of the actinide–amide bond is of kinetic importance in the insertion reaction, which can be viewed as an intramolecular nucleophilic attack on coordinated carbon monoxide. As in the case of organoactinide η^2-acyl complexes,[6,7] some of the properties of the dihaptocarbamoyls can be understood in terms of resonance hybrids with oxycarbenoid character (S).

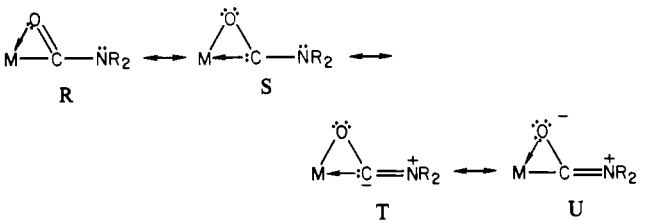

However, the metrical, spectroscopic, and chemical data indicate that resonance hybrid S is of lesser importance for the carbamoyls and that hybrids such as T and U which describe delocalization of nitrogen lone-pair electron density onto the "carbenoid" carbon play a major role in the bonding. Indeed, this π-dative-bonding contribution appears to be significantly greater than in organic amides and probably in transition-metal η-carbamoyls as well. Similar heteroatom effects have been identified in transition-metal carbene complex chemistry.[46a,c] In comparison to organoactinide acyls, we show elsewhere[19c] that this stabilization of the carbenoid center has major consequences for chemical reactivity.

Beyond metal–dialkylamide chemistry, the present results bear upon several problems in the carbon monoxide chemistry of actinide and possibly transition-metal hydrocarbyl compounds. The structure(s) of **7a** have stereochemical implications for the mechanism of CO activation by $M(C_5H_5)_2R_2$ compounds. Although structure D is most compatible with molecular orbital considerations for M = a transition metal,[4c,63] only d-element products of structure E have been isolated[4b] (D may possibly be a fleeting intermediate when M = Zr and R = certain hydrocarbyl functionalities[54]). The present results show that some $M[\eta\text{-}(CH_3)_5C_5]_2R_2$ insertion products can exist in either configuration D or E, that these configurations differ in metrical features and in energy content to only a minor extent, and that the potential energy surface connecting D and E can be rather shallow. In regard to comparing transition metals and actinides, it should be noted that distinct similarities in metal–ligand bonding have recently been found in UPS studies of $M[\eta\text{-}(CH_3)_5C_5]_2R_2$ compounds where M = Zr, Th, and U and R = CH_3 and Cl.[64]

We have previously observed that bis(pentamethylcyclopentadienyl)thorium and -uranium dialkyls undergo rapid and quantitative carbonylation to yield, as the final products, enediolate derivatives[6,7] (eq 13). In the case of fairly bulky alkyl groups

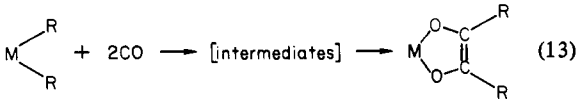

(13)

(e.g., R = $CH_2C(CH_3)_3$, $CH_2Si(CH_3)_3$) the C—C double bond fusion is exclusively intramolecular. Similar results have been reported for M = Zr and R = CH_3.[4a] Although a bis(η^2-acyl) complex V is, a priori, a plausible intermediate on the reaction coordinate from bis(hydrocarbyl) to enediolate, it has so far proven impossible to isolate or to unambiguously implicate such a species.

(61) *Spec. Publ.—Chem. Soc.* **1965**, *18*, M665.

(62) Rosenthal, A.; Wender, I. In "Organic Syntheses via Metal Carbonyls", Wender, I.; Pino, P., Eds.; Wiley: New York, 1968; pp 405–466. Carbamoyl formation via nucleophilic attack of external NR_2^- on coordinated CO is, of course, well documented.[41]

(63) For actinides, it should be noted that the $5f_{z^3}$, $5f_{z(x^2-y^2)}$, $5f_{xz^2}$, $5f_{xyz}$, and $5f_{yz^2}$ orbitals are also of the proper symmetry and spatial orientation for MR_2 σ and π bonding.[64]

(64) (a) Fragalà, I.; Marks, T. J.; Fagan, P. J.; Manriquez, J. M. *J. Electron Spectrosc. Relat. Phenom.* **1980**, *20*, 249–252. (b) Ciliberto, E.; Condorelli, G.; Fagan, P. J.; Manriquez, J. M.; Fragalà, I.; Marks, T. J. *J. Am. Chem. Soc.*, in press.

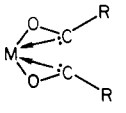

V

It was anticipated at the outset of the present work that the additional steric bulk provided by dialkylamide substituents (R = NR_2) as well as possible electronic stabilization accruing from π-dative interaction with the nitrogen lone pair might well stabilize a bis(η^2-carbamoyl) complex sufficiently to allow isolation or at least observation. The syntheses and characterization of compounds **10a**, **10b**, and **11a** show unambiguously that this approach is possible and that organoactinide species with two proximate η^2-carbonyl functionalities exist. From the structural data it would appear that such a molecular configuration is ideally poised for ring closure and enediolate formation but that the process is inhibited by the steric bulk of the *N*-alkyl functionalities and the necessity of twisting the ligands about C–N bonds with appreciable multiple bond character (as judged by bond distance and the barrier to rotation). Closely related is evidence from the spectroscopic data suggesting a reduction in the carbenoid character of the C–O functionalities in the actinide carbamoyls (relative to the acyls). There are, however, two other factors, of as yet unquantified importance, which may further hinder ring closure. First, the open bis(carbamoyl), bis(carbenoid) complex may actually be thermodynamically more stable than the closed diaminoenediolate. Reactions are known where metal ions insert into the C=C double bonds of electron-rich olefins to form bis(carbene) complexes[65] (e.g., eq 14). Such considerations are

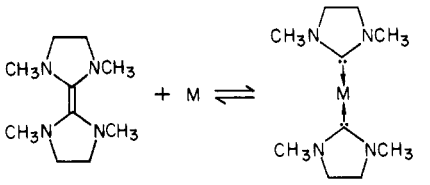

(14)

undoubtedly less important for a bis(η^2-acyl). The second factor is kinetic in nature, is applicable to both acyls and carbamoyls, and reflects the fact that orbital symmetry conservation places constraints upon the mutual orientations from which free carbenes can couple thermally to form olefins.[66] The immobilization in the bis(carbamoyl) introduced by the η^2 ligation, the C–N multiple bond character, and the prodigious intramolecular steric congestion as well as the compensatory effects which may be imparted by the metal ion d and f orbitals are difficult to assess with the data presently at hand. Further investigations of this problem are in progress.

Acknowledgment. We thank the National Science Foundation (T.J.M., Grants CHE76-84494 A01 and CHE8009060) and the University of Nebraska Computing Center (V.W.D.) for generous support of this work.

Supplementary Material Available: Anisotropic thermal parameters for nonhydrogen atoms (Tables IV and IX), detailed experimental descriptions of the X-ray crystallographic studies, and structure factor tables (40 pages). Ordering information is given on any current masthead page.

(65) (a) Cetinkaya, B.; Dixneuf, P.; Lappert, M. F. *J. Chem. Soc., Dalton Trans.* **1974**, 1827–1833 and references therein. (b) Hitchcock, P. B.; Lappert, M. F.; Ferreros, P.; Wainwright, K. P. *J. Chem. Soc., Chem. Commun.* **1980**, 1180–1181.

(66) Hoffmann, R.; Gleiter, R.; Mallory, F. B. *J. Am. Chem. Soc.* **1970**, *92*, 1460–1466. We thank Professor R. Hoffmann for a stimulating discussion of this subject.

Characterization of Cationic Rhodium Isocyanide Oligomers in Aqueous Solutions

I. S. Sigal and Harry B. Gray*

Contribution No. 6282 from the Arthur Amos Noyes Laboratory, California Institute of Technology, Pasadena, California 91125. *Received August 4, 1980*

Abstract: The tetranuclear complex $(Rh_2(bridge)_4)_2^{6+}$ (or Rh_4^{6+}) (bridge = 1,3-diisocyanopropane) forms 1:1 and 1:2 complexes with $Rh_2(TMB)_4^{2+}$ (TMB = 2,5-dimethyl-2,5-diisocyanohexane) in aqueous 1 N H_2SO_4 solution at 25 °C. The formation constant of $Rh_2(TMB)_4Rh_4^{8+}$ is 1.5×10^7 M^{-1} (λ_{max} = 785 nm), and that of $Rh_2(TMB)_4Rh_4Rh_2(TMB)_4^{10+}$ is 4.5×10^{13} M^{-2} (λ_{max} = 980 nm). The hexanuclear complex dimerizes, the formation constant of the dodecanuclear cation ($\lambda_{max} \sim$ 1350 nm) being 1.8×10^4 M^{-1}. Air oxidation of $Rh_2(TMB)_4Rh_4Rh_2(TMB)_4^{10+}$ gives the "mixed" tetranuclear complex, $Rh_2(TMB)_4Rh_2^{6+}$. The intense band (ϵ(Rh) in the range $(2–3) \times 10^4$ M^{-1} cm^{-1}) observed in the electronic absorption spectrum of each of the oligomers is attributable to a $\sigma \rightarrow \sigma^*$ transition; the transition energy decreases systematically with increasing rhodium chain length. Electronic structural relationships of certain of the rhodium oligomers to *cis*-diammineplatinum α-pyridone blue are discussed briefly.

It is well established that certain planar isocyanide complexes of Rh(I) and Ir(I) form dimers, trimers, and even higher oligomers in concentrated solutions.[1-3] Elucidation of the nature of the metal–metal interactions in these oligomers has been facilitated by our work[4-10] on discrete binuclear complexes containing the

(1) Mann, K. R.; Gordon, J. G., II; Gray, H. B. *J. Am. Chem. Soc.* **1975**, *97*, 3553.
(2) Mann, K. R.; Lewis, N. S.; Williams, R. M.; Gray, H. B.; Gordon, J. G., II *Inorg. Chem.* **1978**, *17*, 828.
(3) Geoffroy, G. L.; Bradley, M. G.; Keeney, M. E. *Inorg. Chem.* **1978**, *17*, 777.
(4) Smith, T.; Gray, H. B. "Abstracts of Papers", 180th National Meeting of the American Chemical Society, Las Vegas, NV, Sept 1980; American Chemical Society: Washington, DC, 1980; INOR 173.
(5) Lewis, N. S.; Mann, K. R.; Gordon, J. G., II; Gray, H. B. *J. Am. Chem. Soc.* **1976**, *98*, 7461.
(6) Miskowski, V. M.; Nobinger, G. L.; Kliger, D. S.; Hammond, G. S.; Lewis, N. S.; Mann, K. R.; Gray, H. B. *J. Am. Chem. Soc.* **1978**, *100*, 485.

0002-7863/81/1503-2220$01.25/0